Experimental and analytical investigation of the gamma irradiation effect on the fracture behavior of hip joint bone

By:

Nabi Ahmad

19-FET/MSME/F14

Supervised By:

DR. RAFIULLAH KHAN

DEPARTMENT OF MECHANICAL ENGINEERING,

FACULTY OF ENGINEERING AND TECHNOLOGY

INTERNATIONAL ISLAMIC UNIVERSITY,

ISLAMABAD

MS
GIO
NAE

Gamma Radiation.

Bovine's hipbone.

Thesis entitled

Experimental and analytical investigation of the gamma irradiation effect on the fracture behavior of hip joint bone

Submitted to International Islamic University, Islamabad

In partial fulfillment of the requirements

for the award of degree of

MASTER OF SCIENCE

IN

MECHANICAL ENGINEERING

BY

Nabi Ahmad

19-FET/MSME/F14

SESSION 2014-2016

DEPARTMENT OF MECHANICAL ENGINEERING

INTERNATIONAL ISLAMIC UNIVERSITY,

ISLAMABAD

DECLARATION

I, **Mr. Nabi Ahmad**, Reg.No. **19-FET/MSME/F14** student of MS mechanical engineering in Session 2014-2016, certify that research work titled "Experimental and analytical investigation of the Gamma irradiation effect on the fracture behavior of hip joint bone" is my original research work. The work has not been published anywhere for assessment. Where materials of others involved from other sources has been properly acknowledged and indicated clearly.

Signature of student: _____

Dated: 17/05/2017

Certificate of Approval

This is to certify that the work contained in this thesis entitled, **"Experimental and analytical investigation of the Gamma irradiation effect on the fracture behavior of hip joint bone"** was carried out by **Nabi Ahmad Registration No. 19-FET/MSME/F14,** it is fully adequate in scope and quality, for the degree of MS (Mechanical Engineering).

Viva Voice Committee

Supervisor

Dr. Rafiullah Khan
Assistant Professor
DME, FET, IIU, Islamabad

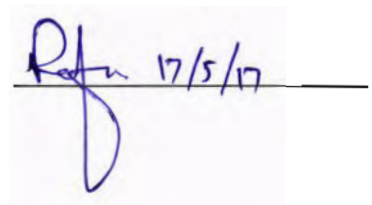

Internal Examiner

Dr. Saeed Badshah
Head of department (HOD)
Associate Professor
DME, FET, IIU, Islamabad

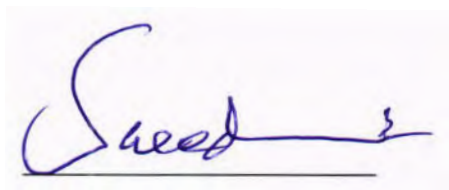

External Examiner

Dr. Asif Israr
Head of department (HOD)
Mechanical Engineering
Institute of Space Technology, Islamabad

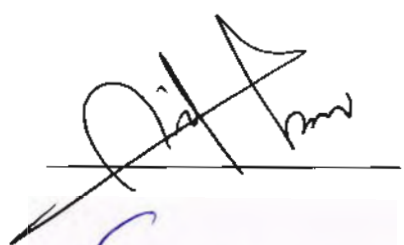

Chairman DME FET IIU, Islamabad

Dr. Saeed Badshah Associate Professor

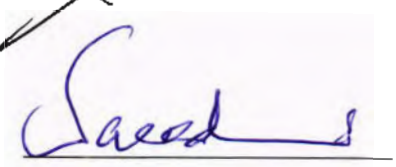

Dean FET, IIU Islamabad

Prof. Dr. Aqdas Naveed Malik

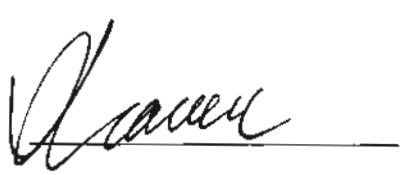

DEDICATION

I dedicate this research work to my family for their patience, kindness and love in my life. I also dedicate it to my father who earned an honest living for us, to my mother a strong, gentle and caring , to my daughter Maham a joy & laughter of my life and to my younger brother Engr. Sadiq Ahmad who answer the call for help with no expectation of personal gain.

ACKNOWLEDGEMENTS

First and above all, I praise God, the most gracious and merciful for giving the opportunity and blessing me to complete the thesis successfully. This thesis is the outcome of the assistance and guidance of several people. I would therefore like to offer my special appreciation to **Dr. Rafiullah Khan**, for his supervision and his warm support, guidance, giving critical comments of the thesis. I want to express my deep thanks to **Dr. Mazhar Mehmood** from PIEAS for the trust, extraordinary generosity, for his support during the entire period of the experimental work and technical assistance in Lab, and especially for his endurance and leadership during experiments.

My parents, I greatly appreciate your excellent assistance and your spiritual supports in all aspect of life to me and to my family during my M.S study. I also appreciate the financial support of Engr. Sadiq Ahmad my younger brother during my M.S study. I also dedicate it to a little angel , my daughter a joy and laughter of my life.

My appreciation goes to my lovely wife, Meena, without her encouragement love and care, and also she stood by me through the good times and bad.

To those who in some way helped and contributed in this research, your thoughtfulness means a lot to me. Thank you very much.

ABSTRACT

Bone is a natural composite anisotropic material composed of mainly three materials, organic, inorganic and water. Bones gives structural support to the body, withstands stresses during movements, lifting heavy loads during fast running.

Each hip bone is combination of three bones merged to one another to form a single bone, the ilium, ischium, and pubis. The hip bone has the most weight bearing capacity joint in the body and so transmits body weight to femur. The hip bone has a structure of ball and socket joint that permits the upper leg to move face to rear and side to side.

The products of bone banks play significant role in covering bone defects during surgical procedure intended at improving the mobility of patients, and minimizing the disability linked with bone and joint diseases. However, using of bone allografts carry a risk of transfer of microorganisms and viruses from giver to receiver. In tissue processing, many bone banks for many years believe it necessary for allografts to be fatally sterilized by means of gamma irradiation from Cobalt 60 sources or X-ray. The mechanical properties of the bones changes with gamma irradiation dose. Literature review shows that mechanical properties of cortical and femur bones changes with gamma irradiation. The literature further reveals that the consequences of gamma irradiation on hip bone are less investigated.

The aim of this thesis was to examine the effects of gamma irradiation on fracture toughness, young modulus and ultimate strength of bovine's hipbone. The above properties were experimentally investigated using samples of hipbone from same age of male bovine. American society for testing and materials ASTM E-399 were used to investigate fracture toughness while tensile strength and young modulus were investigated using ASTM D-3039. The strain fields at the crack tip of compact tension CT specimens were examined using digital image correlation technique. The image files obtained during the DIC analysis were analyzed using software Vic-2D, 2009.

The result shows that fracture toughness, young modulus and strength were decreased with gamma irradiation. It is recommended that the mechanism of the effect of gamma irradiation may be investigated.

Table of Contents

List of Figures

List of Tables

List of Abbreviations

ASTM:	American Society for Testing and Materials
CT SCAN:	Computerized Tomography Scan
CT:	Compact Tension
DIC:	Digital Image Correlation
FEM:	Finite Element Modeling
HA:	Hydroxyapatite
LCT:	Longitudinal Compact Tension
TCT:	Transverse Compact Tension
MRI:	Magnetic Resonance Imaging
TM:	Universal Testing Machine
LT:	Longitudinal Tensile
TT:	Transverse Tensile
EMF:	Electromagnetic Field
3D:	Three dimensional
TA-GVHD:	Transfusion Associated Graft Versus Host Disease

Chapter 1

INTRODUCTION

1.1. Bone

Bones gives structural support to the body. It works as connective tissue that has the potential to repair and regenerate, comprised of a firm medium of calcium salts deposit around protein fiber. The mineral portion of bone provides rigidity while the proteins provide elasticity. Bone tissue are categorized mainly into two types, cortical and trabecular bone, have the ability to withstand considerable stress throughout the actions and tiring activities such as lifting weighty stuffs or quick running [1].

At the nano level, bone tissue is formed by combining inorganic, organic phase and water. On the basis of weight, bone is just about 60 % inorganic, 30 % organic, and 10 % water [2]. The inorganic portion of bone includes ceramic crystalline type mineral that is a contaminated form of calcium phosphate in nature, the majority often known as hydroxyapatite ($Ca_{10}(PO_4)_6(OH)_2$) [3]. Bone hydroxyapatite is not clean hydroxyapatite because the minute apatite crystals of long plate's size 2 to 5 nm thick × 15 nm wide × 20 to 50 nm have impurities such as magnesium potassium, carbonate, sodium, strontium, and fluoride or chloride. The organic portion of bone consists mainly of type I collagen, some other types III and VI collagen, and a mixture of noncollagenous proteins such as osteonectin, osteopontin, osteocalcin and bone sialoprotein [4]. The collagen molecules are prearranged with each other in parallel from top to end with a opening or "hole zone" of roughly 40 nm between each molecule [5]. The process of mineralization take place in the hole zone and extend into the spaces between molecules, resulting in the mineralization of fibril. The 3D collection of collagen molecules inside a fibril is not sound understood. However, the diameter of collagen fibrils in bone vary from 20 to 40 nm, suggestive of that there are 200 to 800 collagen molecules in the cross section of a fibril. The microstructure of bone have four levels comprised of mineralized collagen fibrils, lamellar woven, primary lamellar woven to cortical and trabecular bone are shown in Figure 1.1 [6].

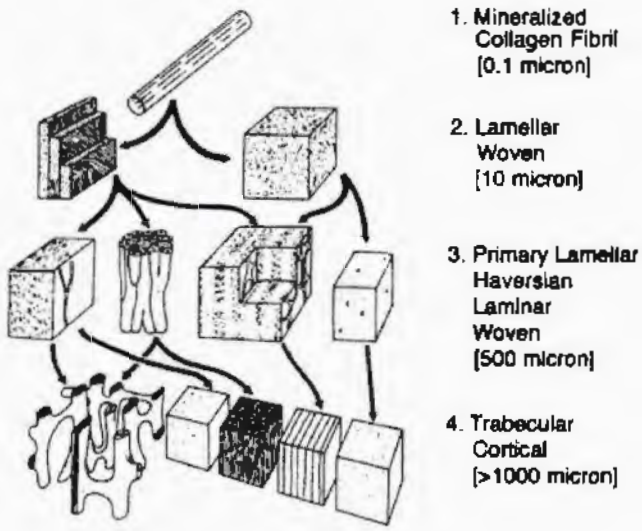

Figure 1.1: The four levels of bone microstructure[6].

1.2. Hip bone

Each hip bone is shaped by three bones merged to one another to form a single bone as shown in Figure 1.2. The ilium is the superior, the ischium is inferior and posterior, and the pubis is inferior and anterior. The hip bone joins interiorly at the symphysis pubis. Posteriorly, each hip bone joins the sacrum at the sacroiliac joint. A fossa called the acetabulum is positioned on the side surface of each hip bone. The acetabulum is the spot of articulation of the lower limb with the pelvic girdle. Lower to the acetabulum is the big obturator foramen. The front portion of the ilium is called the iliac crest. The crest ends interiorly the same as the anterior superior iliac spine and on the back side as the posterior superior iliac spine [7].

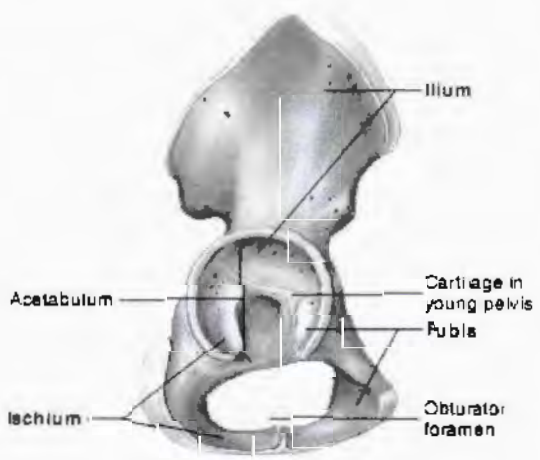

Figure 1.2: Hip bone [7].

1.3. Problem statement

Bone allograft is irradiated for sterilization purpose using gamma or X- rays. Irradiation effects bone properties. The literature review reveals that in the past the behavior of various bone types has been studied for the assessment of irradiation effect using three point bending test, compression testing, fatigue and flexural testing. However least work has been worked out for the effect of gamma irradiation on the hip joint bone. It is a fact that the composition and the structure of bone varies with its location in the skeleton site. Being an important bone, investigation of hip joint bone with irradiation effect is of prime importance.

1.4. Motivation of research & its impact on society

Bone banks contribute to broad range of tissue, including massive bone allografts cortical bone allografts. During bone transplant these products helps to improve patient's movement and also it reduces the disability associated with diseases of joints and bones. Whenever bone allografts are used there is possibility of transferring bacteria, viruses from donor to recipient. To avoid possible infection, donor screening is important along with surgical sterilization. In the process of sterilization many bone banks consider it necessary for allografts to be cleaned with the help of gamma irradiation of source Cobalt 60 in such range that its mechanical properties remains same after irradiation.

1.5. Objective of the research

The primary objective of this thesis is to examine the effect of gamma irradiation on fracture toughness of the bovine hip cortical bone. The secondary objectives are to look into the effect of gamma irradiation on the following mechanical properties of the hip bone

i. Young modulus
ii. Ultimate tensile strength

1.6. Research methodology

The research has been carried out experimentally and analytically. The analytical section includes the investigation of the stress field at the cracks in the bones. Analytical analysis has been done using fracture mechanics approach. The displacement field or the strain distribution at the crack tip has been studied using digital image correlation (DIC) while using Vic-2D, 2009.

1.7. Thesis layout

Next chapter describes the bone composition and its types. Chapter 3 describes detail of radiation, its types and the equipment for gamma irradiation. Chapter 4 is the literature survey of previous work on gamma irradiation effects on bone properties. Chapter 5 describes the experimental details. The results of the experiments are discussed in chapter 6. In last chapter conclusions and further recommendations are summarized.

Chapter 2

BONE STRUCTURE

This chapter contains the details of bone, its structure and types of bone. First section introduces and discusses the composition of bone. Types of bones are discussed in section two.

2.1. Bone

The bone is responsible for providing both structural supports as well as it protects the organs of the body. It gives protection to the brain, spinal card. It also forms the framework which supports the body and works as a levers to move the body and its parts [8-9]. The bones works as a reservoir for some mineral [10-11] e.g. calcium and phosphorous. Bone has the ability of regeneration and repair [12].

2.2. Composition of bone

Bones are composed of two solid materials [13]. Biological tissues such as bone are listed in the category of natural composite material [14], which are not artificial or manmade composites materials but appears to be as it is in nature.

Bone is compared hierarchically at nano scale to a composite material. Bones are composed of type I collagen fibers which are toughened with calcium phosphate crystals. Bone contained water 25% of its weight, located within blood vessels in harversian canals. The inorganic portion of bone is composed of carbonated apatite i.e. (Ca_5 (PO4)3, (OH)), which are having crystal type shape. In case of dry bone these crystals are present up to two third of the weight of bone. The remaining portion of the weight corresponds to organic material, which is collagen, also lipids and non collagen proteins. Collagens are responsible for absorption of energy i.e. for toughness, whereas for stiffness the mineral portion is responsible. The collagen, mostly containing protein in mammals and is formed by molecules that have a length approximately of 280 to 300 nm and a diameter of 1.5 nm. The collagen molecule is the composition of three polypeptide chains, which form a triple helix molecule [15].

The bone is also a brittle material. The brittleness of the bone depends on the mineral portion that gives it the capability to support compressive loads. The bone tissue is a viscoelastic material whose mechanical properties are affected by its deformation grade. The collagen material of the bone provides the flexibility properties to the bone [16].

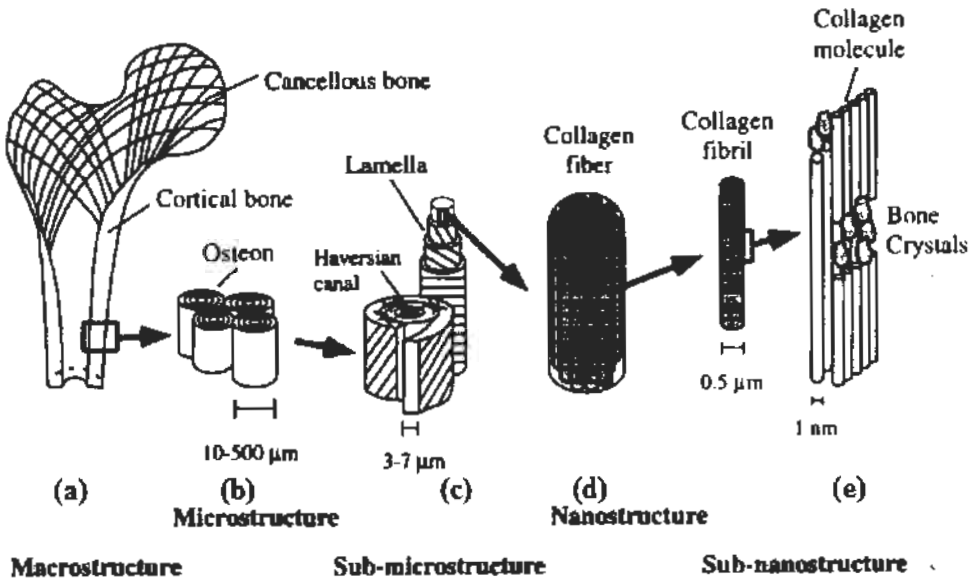

Figure 2.1 : Hierarchical structural organization of bone: (a) cortical and cancellous bone; (b) osteons with Haversian systems; (c) lamellae; (d) collagen fiber assemblies of collagen fibrils; (e) bone mineral crystals, collagen molecules, and non collagenous proteins [17].

2.3. Types of bone

The bones are classified into four major types of bones and then it is further divided into sub groups as shown in the Figure 2.2.

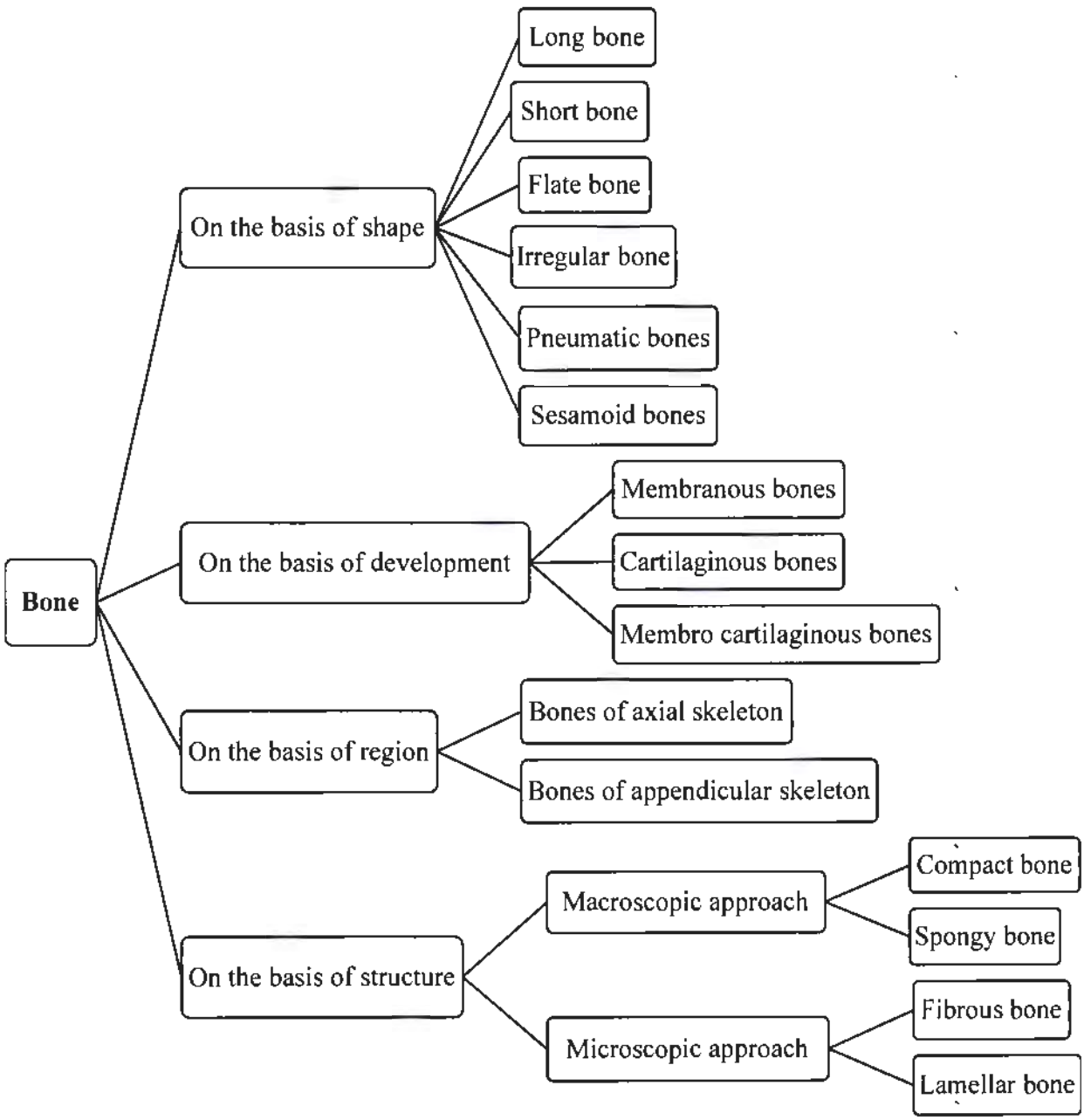

Figure 2.2: Classification of bones.

2.3.1. Cortical or compact bone

Compact bone tissue forms the external shell of the bone. It is very hard and thick. It appears solid to unaided eye. This type of bone holds closely packed cylinders of bone harden by calcium carbonate known as osteons. Osteons mainly comprise of lamellae's concentric layers, which are arranged in such a manner that seems to be drinking straws. In the center of the

osteons there are longitudinal canals that have blood vessels, nerves and lymphatic vessels. At right angle to central canal there are branches known perforating canals which extends the nerves system and vessels out ward to periosteum and to endosteum. Lacunae contained in lamella which means little spaces houses osteocytes (bone cells). From each lacuna there are small canaliculi where nutrients and wastes can pass to and from central canal is the extension of the osteocytes. The human Skeleton contains 80 % cortical bone by weight. These bones are compact in shape. It is located in the shaft of long bone like femur is typical example of the cortical bone. It structure contains 5-10 % of porosity. It has slow circulation of nutrients and wastes.

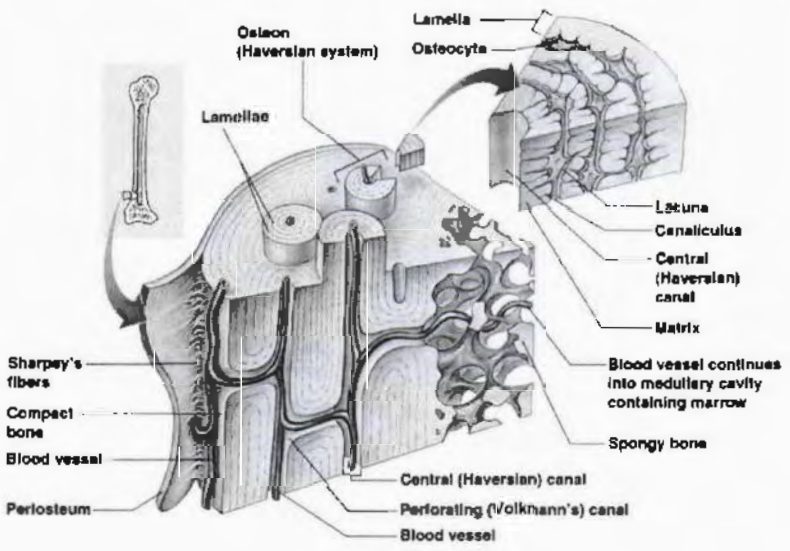

Figure 2.3: Structural arrangement of cortical and cancellous bone [18].

2.3.2. Cancellous or spongy bone

Cancellous bone is also known trabecular bone or spongy bone. This type of bone is found in the axial skeleton of the vertebral bodies and in the appendicular skeleton it is located in the end of the long bones. The spongy bone has a complex, porous and maximum strength for smallest mass of the skeleton and as a whole it is arranged in space [19]. This type of bone has more surface area and is less dense than compact bone. Due to higher surface area these bones have more metabolic activity e.g. exchange of calcium ions. It is composed of a mesh work of inter connecting sections of bone called trabeculae as shown in Figure 2.4. Bone marrow is filled in the spaces between the trabeculae. At microscopic level, cancellous bone composed of plates

and bars. These bars are near to, irregular cavities containing red bone marrow. Although these plates are arranged in irregular manner but it gives more strength like building braces. These bones contain red bone marrow and that's why it produces blood cells [20].

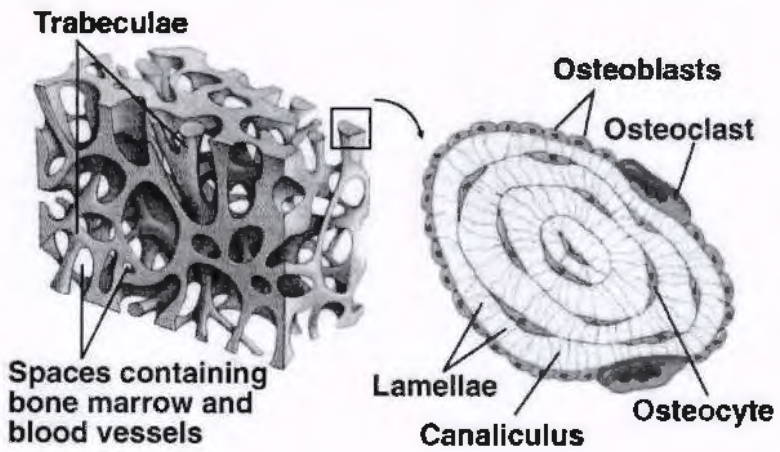

Figure 2.4: Structural arrangement of cancellous bone [18].

2.3.3. Femur

This is the major bone of the upper leg and is also known none medically as the 'thigh bone' as shown in Figure 2.5. This bone is long in shape and rotates between the hip and the knee. The femur has narrow head. Femur bone is known to be the longest, strongest and largest bone of the body. Due to mscles coverage these bones cannot be felt. There is a small, pit called the fovea capitis at the femure head, where the ligamentum teres helps to secure the head into the acetabulum [21].

Figure 2.5: Femure structure [22].

2.3.4. Tibia

The tibia is also called the 'shin bone' and this is the inner and larger bone of the lower leg as shown in the Figure 2.6. The tibia articulates with the femur above, the ankle bones

below, and the fibula at the ends. This type of bone supports body weight, transferring between femur and talus [21].

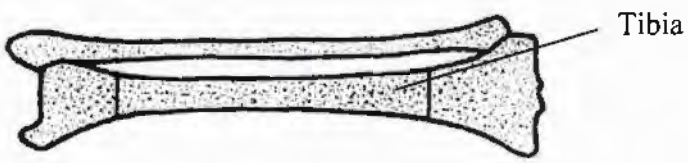

Figure 2.6: Tibia structure [23]

2.3.5. Hip bone

The hip bone has a structure of ball and socket joint that permits the upper leg to move front to back and side to side. The hip bone has the most weight bearing capacity joint in the body and so transmits body weight to femur. This is asymmetrical bone formed by merging of ilium, ischium, and pubis which are different from each other in structure. The hip bone is constricted in the centre and expanded above and below as shown in Figure 2.7 [21].

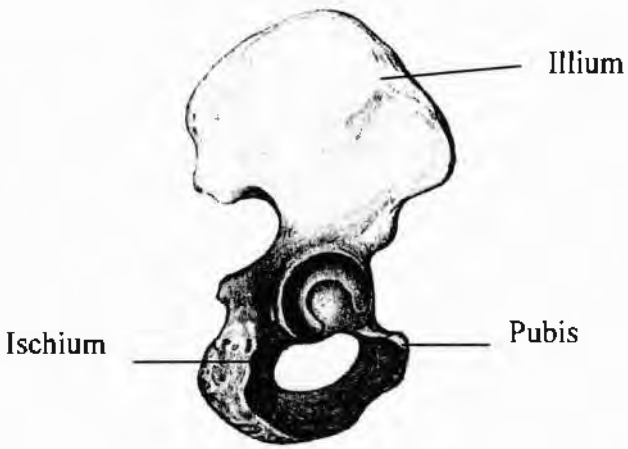

Figure 2.7: Hip joint bone structure [24].

2.3.6. Patella

The shape of this bone is triangular sesamoid bone packed in the patellar tendon as shown in Figure 2.8. The quadriceps femoris muscle to the tibia is attached by patellar tendon. There are two surfaces Patella bone; the one which is rounded is a convex anterior surface, and the smooth, articular posterior surface. This bone acts to increases leverage for quadriceps muscle by keeping some gap between tendon and the axis of rotation [21].

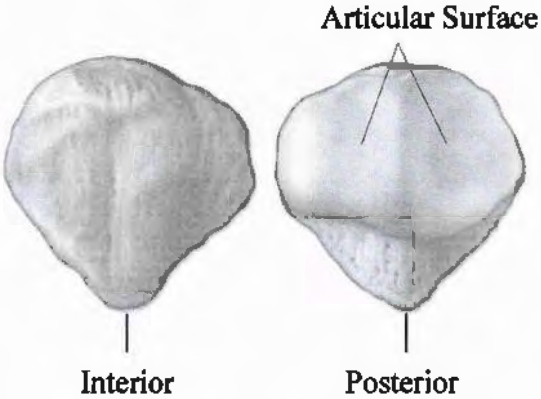

Figure 2.8: Structure of patella [25].

The test results of the fracture toughness and tensile experiments are presented and discussed in the next chapter.

Chapter 3

RADIATION

This chapter presents an introduction to ionizing radiation. The chapter discusses the nature of radiation, how it is produced, and its properties. The use of radiation in bone allograft is discussed in the last section.

3.1. Introduction

Radiation is the form of energy or particulate matter which travels as electromagnetic waves and composed of atoms and molecules. These atoms are bound into molecules by electrons. There are two types of atoms stable and unstable. Stable atoms are not radioactive and unstable atoms have surplus of energy or mass. In order to reach stability these atoms emits the surplus energy. These emissions are called radiations. As a result of this radiation positive charged atoms and negative charged atoms are produced. There are two types of ionization radiations photons i.e. gamma and X-rays, and particles i.e. alpha, beta and neutrons. Unstable atoms emit photon or sub atomic particles to become stable. This process is known as radioactive decay. Instead of how ionized atoms are formed chemically these atoms are more active than neutral atoms. Also the active ions of these atoms form compounds that impede with the processes of cell separation and metabolism. The severity of damages suffered during contact to ionizing radiation depends upon the type, intensity, energy, interval, and chemical type of radiation [26].

3.2. Source of radiation

Solar radiation is the first cause of heat and light. It is source of visible rays, ultra violet rays and infrared rays. Visible rays are used for light; ultra violet rays provide vitamin D and infrared rays gives warming effect. Some manmade devices also produce electromagnetic radiations. Examples of some well known sources are microwave oven, radio and television, transmitter, fluorescent lamp and X- rays machines [27].

3.3. Types of radiation

3.3.1. Alpha particle

Alpha particles decomposition occurs whenever an atom ejects a particle from its nucleus. This particle composed of two neutrons and two protons. By happening this, the atomic number of atom is decreases by 2 and the mass decreases by 4 as shown in the reaction in Figure 3.1. Examples of alpha sources include radium, radon, uranium and thorium. Alpha particle and helium nucleus have the same structure. Alpha particles may be written as shown and they have a double positive charge and a mass of 4 u [28].

$$_{92}U^{238} \xrightarrow{\text{yields}} {}_{2}He^{4}\ (\text{alpha particle}) + {}_{90}Th^{234} \qquad (3.1)$$

Alpha particles when pass through any matter by colliding with its nuclei lose energy and causes ionization. Alpha particles are heavier and more highly charged particles that can be stopped by a thin sheet of paper or plastic. These particles are hazardous to health when inhaled.

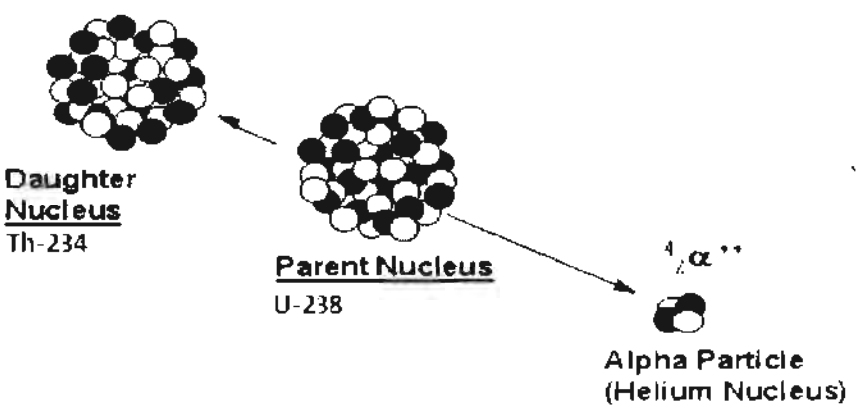

Figure 3.1: Alpha particle [29].

3.3.2. Beta particle

In case of beta decomposition, the atomic number is increases by one, but the mass only decreases to some extent when neutron is changed into a proton and an electron is emitted from the nucleus. Examples of pure beta sources include carbon-14, strontium- 90, sulphur-35 and tritium. Betas minus particles are electrons as shown in Figure 3.2. Beta minus particles may be written as [30]

$$_{0}n^{1} \xrightarrow{yields} {}_{+1}p^{1} + {}_{-1}e^{0} \qquad (3.2)$$

Beta particles have a negative charge and a mass of 1/1800 u. By colliding with the nuclei of any matter they cause ionization and lose energy when they are passing through beta particles. The lighter beta particles can be stopped by a thin sheet of metal.

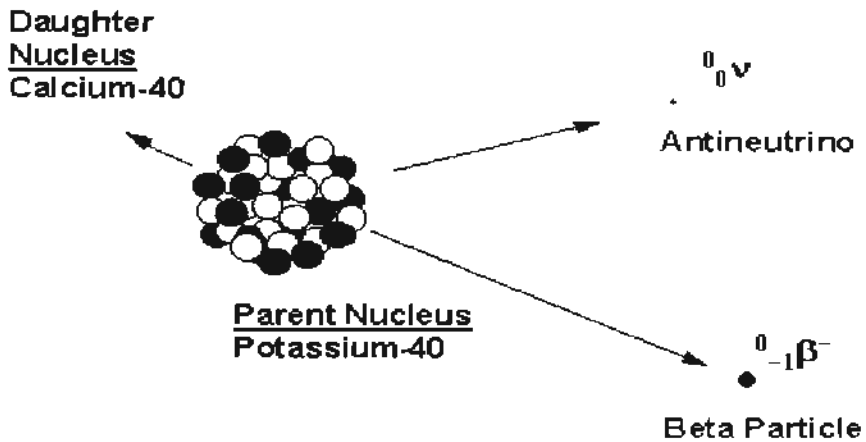

Figure 3.2: Beta particle [29].

3.3.3. Gamma particle

Gamma particles are not particles and are high energy (low wavelength) electromagnetic radiations. This type of radiation does not carry any charge or mass as shown in Figure 3.3. These particles travel with the velocity of light. These are not deflected by electric or magnetic field. They have the highest penetrating power and they can pass through much thicker aluminum sheets. They can be stopped by aluminum sheet of 100 cm thickness. They ionize the gases but to the smallest extent. Without inhalation or ingestion these radiation can therefore carry significant doses to internal organs. To stop gamma radiation and neutrons the thickness of shielding required varies depending on the energy and intensity, but can be several meters of concrete. One or more gamma photons can be emitted from the excited states of daughter nuclei following radioactive decay. When a radioactive nuclide expels alpha or a beta particle in very high speed, it is often excited to a higher energy level. After some time, nuclide comes back to the ground state by emitting one photon of a short wavelength radiation called gamma radiation [31].

$$_{27}Co^{60} \xrightarrow{yields} {}_{-1}e^{0} + {}_{28}Ni^{60**} \text{ (2nd excited state)} \quad (3.3)$$

$$_{28}Ni^{60**} \xrightarrow{yields} {}_{28}Ni^{60*} \text{ (1st excited state)} + \gamma \text{ photon)} \quad (3.4)$$

$$_{28}Ni^{60*} \xrightarrow{yields} {}_{28}Ni^{60} \text{ (ground state)} + \gamma \text{ photon)} \quad (3.5)$$

Thus after the emission of a beta particle by a Co-27 isotope, the new nuclide Ni-60 climbs up to the second excited state. It comes back to ground state in two successive jumps and thereby emits two photons of gamma rays. Examples of gamma sources include cesium-137, iodine-131, cobalt-60, technetium-99 and radium-226.

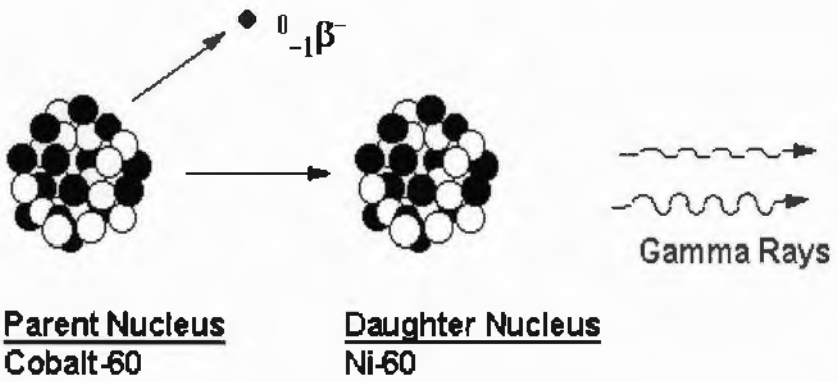

Figure 3.3: Gamma radiations [29].

This type of radiation i.e. gamma radiation release is often associated with alpha or beta decay. It removes energy from an unstable nucleus. The combine penetrating power of all radiation is shown in Figure 3.4 [29].

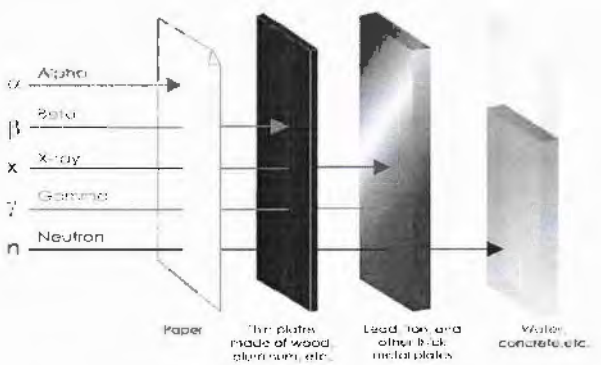

Figure 3.4: Penetrating power of α, β & γ radiation [29].

3.3.4. X-rays

X-rays are known high energy photons that are formed by the interaction of charged particles with matter. X-rays are efficiently produced by the rapid deceleration of charged particles by a high atomic number material. Gamma rays and X-rays have basically the same properties, but they are differing in origin. The processes for X-rays emission is outside the

nucleus, while for gamma rays the process begin inside the nucleus. Generally X-rays are lower in energy and are having less penetrating power than gamma rays. A lead of few mm of thickness can stop medical X-rays. The allocated energy to X-rays is continuous with a maximum energy of about one third that of the electron having more energy. As photons it interacts with matter and due to the transfer of energy their spectral distribution is further changed in a complex manner. X-rays are shown in Figure 3.5 [29].

Figure 3.5: X-rays [29].

3.3.5. Neutron radiation

Neutron radiation composed of a free neutron, usually emitted as a result of spontaneous or induced nuclear fission as shown in Figure 3.6. They can travel in air for hundreds or even thousands of meters, however they are able to be stopped by a hydrogen rich material, such as concrete or water. They are not naturally able directly to ionize an atom due to the lack of a charge, but it ionizes an atom indirectly. They are absorbed into a stable atom, thereby making it unstable and more likely to emit off ionizing radiation of a different type [29].

Figure 3.6: Neutron radiation [29].

3.4. Radiation effects

Radiation effects may be different types of health effects depends on different part of the body, doses sizes, delivery rate of dose and time of radiation exposure. When a given total dose received for a shorter time period it will cause more damage. When the entire body is exposed to very high dose it can causes death within weeks. For example, an absorbed dose of 5 gray or more received instantly would most likely be fetal, unless treatment is given, because it causes damage to the bone marrow and to the gastro intestinal tract. When a person exposed to 5 gray, the life can be saved with medical treatment, but when the whole body is exposed to a dose of 50 gray then it will be fatal even with medical attention.

The physiological effects of radiation are also called somatic in which the radiation immediately affects the body when it is exposed. Death can occur from damage to bone marrow. If this type of effect is belated it can causes cancer, cataracts, leukemia, abortion and life shortening from organ failure [32].

Some genetic effects to off spring if exposed to radiation are harmful and irreversible. The genetic effect may be extended to many generations includes reduction in the probability of survival. Radiations having low penetrating power such as particles are not hazardous to the outside skin if exposed to some radiations, but those radiations that penetrates directly to the tissue such as X-rays, gamma rays, and neutrons, can damage the bone marrow which is blood forming tissue and is dangerous to the body. It also effects the lenses of the eyes and the reproductive organs [33].

Biological effects of non ionizing electromagnetic field on lower organisms have been established, but research on physiological effects on humans is unconvincing and is continuing. Recently, some concerns have been arisen about the possibility of brain tumors caused by using cell phone. The everywhere background radiation originates from a variety of sources including radon; terrestrial radionuclides such as uranium, thorium, and their progeny e.g. cosmic radiation and even radionuclides within our own bodies. Human beings are frequently exposed to different types of radiation e.g. gamma rays, beta particles, and particles from radon and its daughters. The radon gas is always present as a decay product of natural uranium in homes and other buildings. Neutrons as a part of cosmic radiation bombard all living things [33].

3.5. Radiation dose unit

A number of dedicated terms need to be defined to discuss biological effects of radiation. First is the absorbed dose (D), which is the amount of energy imparted (ΔE) to the exposed material mass (m).

$$D = \frac{\Delta E}{m} \tag{3.4}$$

The energy absorbed appears as ionization energy of the molecules or atoms of the medium. The SI unit of dose is the gray (Gy), which is 1 J/kg. An older unit of energy absorption is the rad (radiation absorbed dose), which equals 0.01 J/kg.

3.6. Equipments used for gamma radiation

With the passage and development of the industry, the products to be treated with gamma radiation for different purposes are also increases. In present era the different types of materials are irradiated for different purposes and applications. For the designer the main challenge is to how expose the materials to maximize the utilized energy with dose consistency. The shape, density and composition of new products need modifications in the design. Frozen and chilled foods require special requirements. To cope up this requirement the designers have developed several types of irradiators some of which are described here [32].

3.6.1. Product overlap irradiators

This type of irradiator is used to irradiate the product in metal container. These containers are sometimes also called as totes. Tote irradiators are used in vast range because of the treatment of the goods contained in boxes, bags or drums. The product accommodation capacity of tote is limited to hundreds kg only. These totes are located on roller bed conveyors in four rows two on either side of the source rack and at two levels and it surrounds source of radiation. The totes are shuttles by elevators between consecutive conveyor levels as shown in Figure 3.7. The total height of the source rack is less than that of two totes, which gives result in product overlap and also it helps the dose uniformity in the product. The energy utilized in this type of irradiator is maximum. This irradiator is complex due to the movement of products in two levels [32].

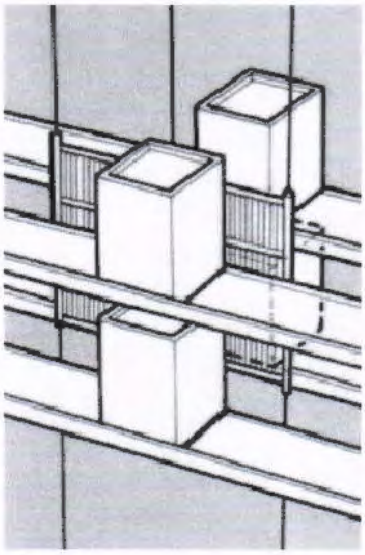

Figure 3.7: Product overlap irradiator [32].

3.6.2. Source overlap irradiators

This type of irradiator has simple transport mechanism of one level, four or more rows for product irradiation as shown in Figure 3.8. The height of the source rack in this case is more than that of container or carrier, and so the arrangement is called source overlap arrangement. These containers are hanged in tracks from ceiling. The total energy in this case of irradiator is less than that of product overlap irradiator but the dose is uniformity level is same for both irradiators [32].

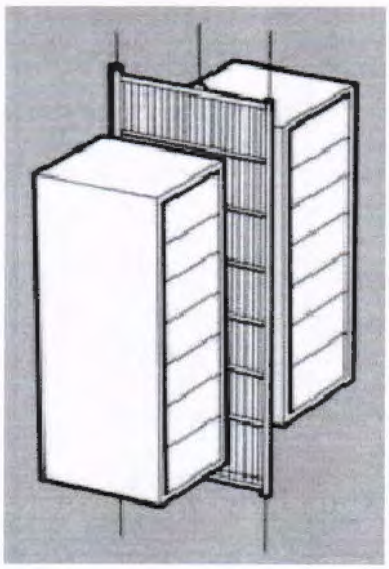

Figure 3.8: Source overlap irradiator [32].

3.6.3. Pallet irradiators

This type irradiator is able to irradiate the whole product at once when the product comes in, in the irradiation facility. The containers in this type of irradiator have standard sizes which can also be used for other activities involved during production process. The design of pallet irradiators is similar to the design of product overlap irradiator. Pallet irradiator has two main advantages over the product overlap irradiator. It saves the extra effort of arranging the product boxes in irradiation container and putting back after irradiation process in pallets for transportation purpose. This irradiator also avoids any damages in handling of products. Pallet irradiator is shown in Figure 3.9 [32].

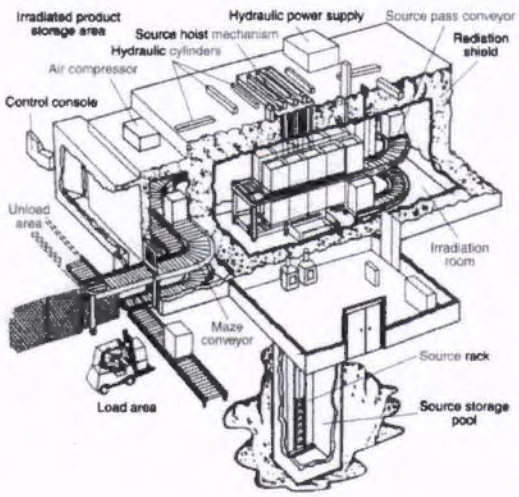

Figure 3.9: Pallet irradiator [34].

3.6.4. Batch irradiators

This type of irradiator is simple and used to small extant of irradiations. The source is shielded and the product containers are placed in arranged manner in the irradiation room. To get the required dose uniformity, each container is exposed to continuous irradiation on a turntable which rotates continuously during irradiation. The containers may revolve one by one around the source as shown in Figure 3.10 [32].

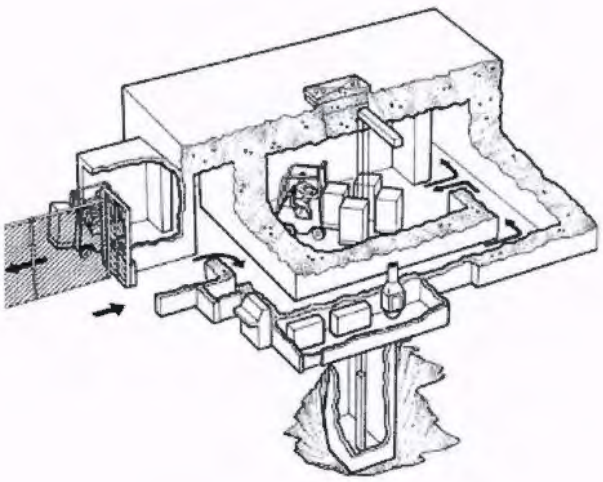

Figure 3.10: Batch irradiator [34].

3.6.5. Self contained irradiators

Self contained irradiators are specially designed for research and applications purposes. This irradiator is used for small doses. In this type of irradiator the dose uniformity ratio should be always smaller than the approved dose limit ratio for the application. This irradiator is used for blood irradiation for preventing TA-GVHD and reproductive sterilization of insects for pest management programmes [32]. The irradiator is shown in the Figure 3.11.

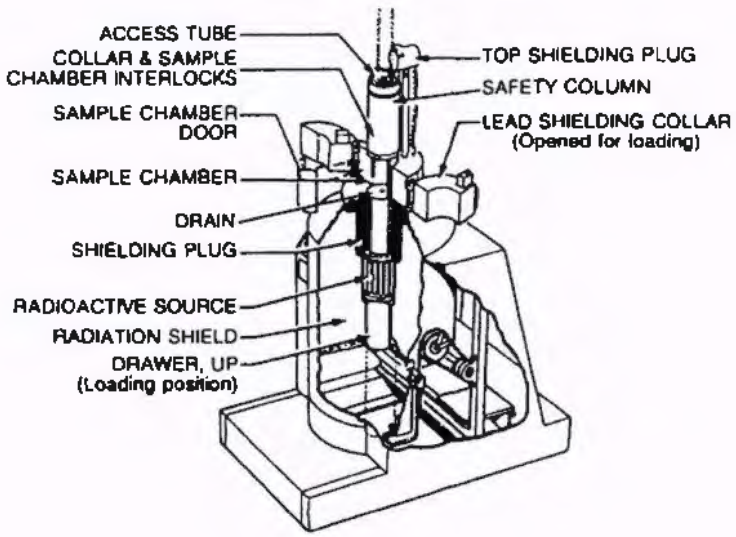

Figure 3.11: Self contained irradiator [34].

3.7. Use of radiation in bone grafting

Bone banks contribute to broad range of tissue, including massive bone allografts cortical bone allografts, and powdered bone. During surgery these products helps to improve patient's movement and also it reduces the disability associated with diseases of joints and bones. Whenever bone allografts are used there is possibility of transferring bacteria, viruses from giver to receiver. To get rid of possible infection, donor screening is important along with surgical sterilized technique from getting of tissue to its processing and storage [35]. In the processing phase of tissue, many bone banks consider it necessary for allografts to be cleaned with the help of gamma irradiation of source Cobalt 60 [36].

Gamma irradiation produced from Cobalt 60 sources has been used for sterilization of bone allograft for many years. When gamma radiation dose is increased above 25 kGy for cortical and 60 kGy for cancellous bone, it causes reduction in mechanical properties due to splitting polypeptide chains [35].

Chapter 4

LITERATURE REVIEW

This chapter covers the literature review of the mechanical behavior of different bones with the gamma radiation dose. The effect of gamma radiation on mechanical properties of several bone types of human beings and bovine has been broadly investigated in the past few decades. The following paragraph describes studies on the radiation effect on fracture toughness, tensile strength and modules of elasticity of femur, tibia, and cortical bones.

Barth et al. [37] characterizes the irradiation effect on structural order and its mechanical properties by examining bone samples from the mid section of the 49 years old male frozen human cadveric cortical bone. Unnotched three point bend test was performed and it was observed in their study that the bone exposed to radiation between 0.05 and 630 kGy gives results in intense decrease in mechanical properties i.e. strength, ductility and toughness, however as the radiation level crossed 630 kGy, the fracture toughness was decreases by a factor of five (5). It was observed that no major mechanical changes took place for irradiation exposure of 35 kGy.

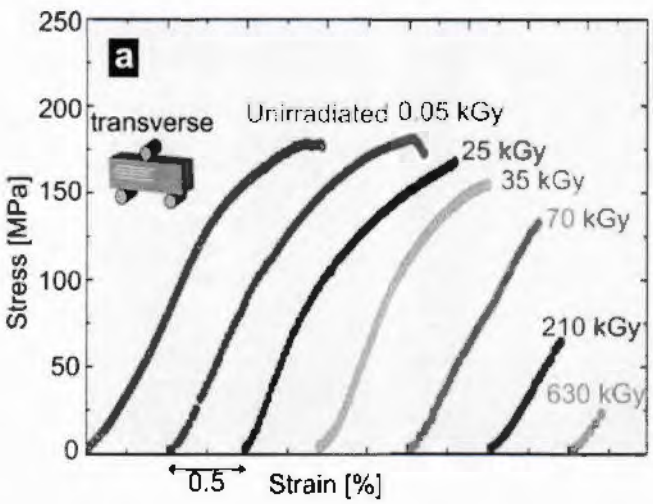

Figure 4.1: Stress strain curve from three point bend testing [37].

Barth et al. [38] investigated the effect of X-ray radiation on deformation and fracture in human cortical bone. The strength, ductility and fracture resistance of human femoral bone in the transverse direction have been studied after exposures to different dose of irradiation. The results showed that the radiation used in tomography imaging of cortical bone can have harmful effect

on the strength, fracture toughness and post yield behavior. Plasticity of the bone was observed to be decreased after 70 kGy of radiation and after 210 kGy of radiation the fracture toughness decreased by a factor of five.

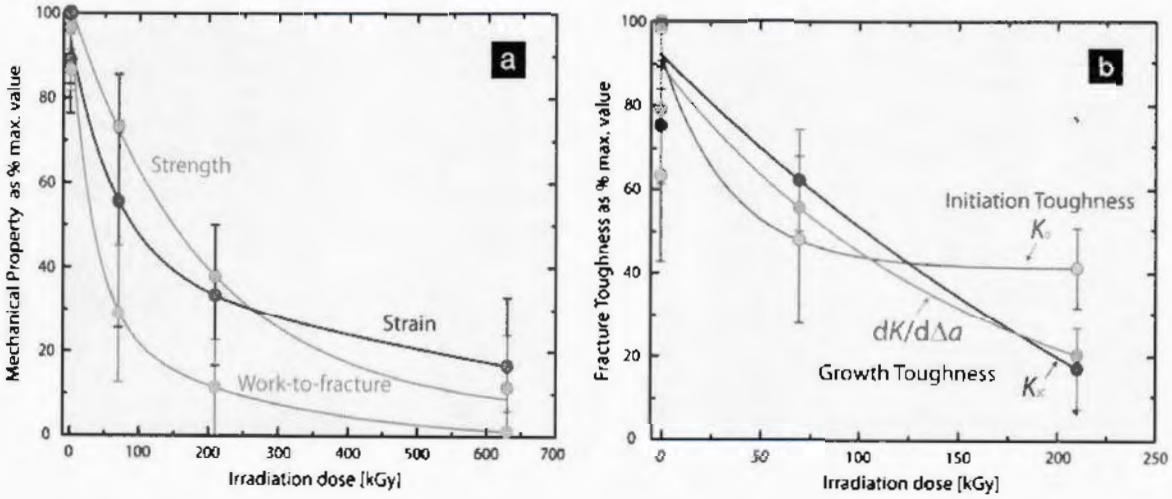

Figure 4.2: a) γ Irradiation effect on ultimate bending stress & strain & fracture toughness & (b) γ Irradiation effect on crack initiation toughness and crack growth toughness.

The graphs illustrates that whenever the X-ray irradiation dose is increases bending stress/strain and toughness decreases gradually [38].

Russell et al. [39] has studied the effect of gamma radiation of two different doses 15 kGy and 25 kGy on the bovine cortical bone. He used calibrated servo hydraulic testing machine to estimate radiation effect on the anisotropy of cortical bone in compression. Different groups, each of fifteen cubes were assigned to radial, axial or tangential testing respectively. Radiation effected collagen and so the ultimate stress and the energy absorbed to failure was reduced [40].

Burton et al. [41] studied that how the bone is embrittlled and the changes in collagen structure due to high dose of gamma irradiation for sterilization. The study was carried out using hydrothermal isometric tension testing and it was confirmed that approximately 33 kGy of gamma irradiation sterilization of bovine cortical bone resulted in considerable loss of bone collagen network. Ultimate stress, failure strain, yield strain and work to fracture decrease were observed using three point bending test, while no difference was detected in modulus, yield stress. Thermal and chemical methods further added that the collagen of bone is modified by oxidation, showing more possibility of increase in collagen network non covalent bonding.

Singhal et al. [42] studied X-rays effect on bovine cortical bone for elastic properties and residual strain at nanoscale. The X-rays dose range of 5-3880 kGy was used to break out the collagen interface. It was determined that residual strain of the bone was decreased with fatigue loading. The apparent moduli of HAP and strain remained unaffected to radiation dose of up to 3836 kGy. It was observed that least residual strain in compression with increase in radiation doses, and vice versa in the fibrils. These observations were considered the main cause of interfacial de bonding of HAP collagen initially strained due to loading and irradiation.

Gibbons et al. [43], on the basis of optical surface strain analyses investigated the effect of gamma radiation on the stress, strain bending strength of goat pateller tendon bone allografts. It has been observed below 30 kGy of radiation that there is no reduction in compression, torsional, and bending strength but the maximum stress and strain energy density of human bone was decreased.

Tu¨fekci et al. [44] studied the effects of gamma irradiation at room temperature for 30 kGy for high strain rate compressive behavior of equine cortical bone. The quasi static results showed that with gamma irradiation there was 9% reduction in ultimate strength, 27 % ultimate strain and 41%, fracture toughness. This study also revealed that there was no effect on modulus of elasticity, resilience and yield strain. It was observed in quasi static loading that whenever the dose of gamma irradiation is increases under high speed loading, the modulus of elasticity, ultimate strength and toughness decreases and vice versa for non irradiated bone.

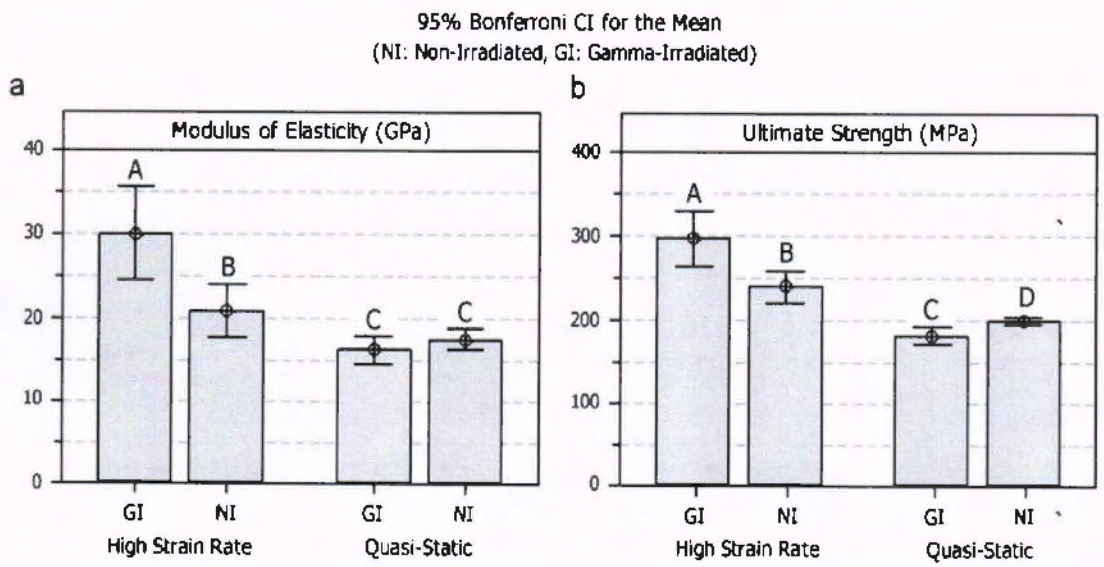

Figure 4.3: Bar charts showing the modulus of elasticity (a), ultimate strength (b) [44].

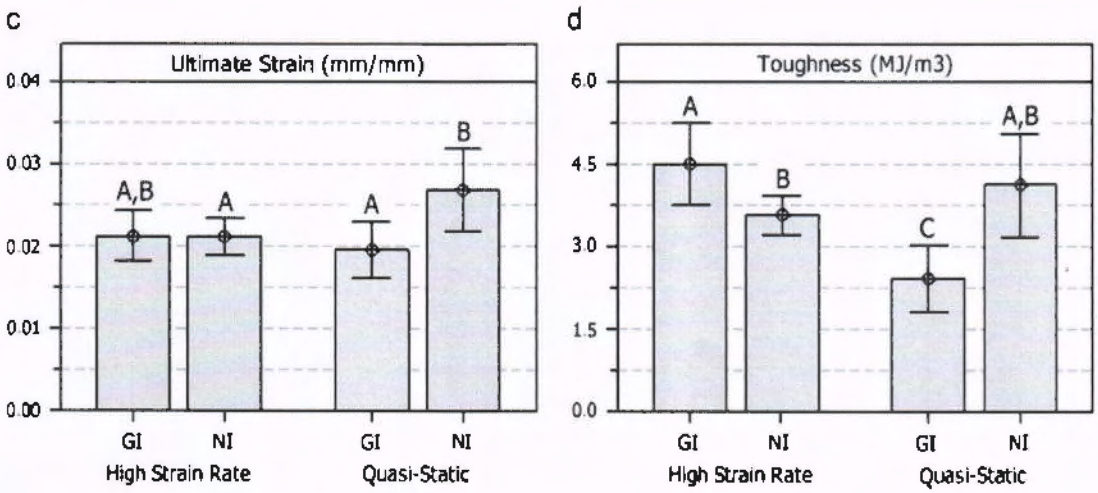

Figure 4.4: Bar charts showing the modulus of ultimate strain (c), fracture toughness (d) [44].

Balsly et al. [45] used two dose ranges of 18.3–21.8 kGy and 24.0–28.5 kGy to investigate the effect on two familiar bone grafts Cloward dowels and iliac crest wedges and four common spongy tissue grafts patellar tendons, anterior tibialis tendons, semiten dinosus tendons, and fascia lata and soft tissue allograft using conventional compressive and tensile testing. For dose range of 18.3–21.8 kGy and 24.0–28.5 kGy no effect was observed on the strength and elastic modulus of any allograft. The Patellar tendon has no change in modulus of elasticity but it loses its tensile strength. The elastic modulus of fascia is decreases and its tensile strength remains same after radiation dose.

Akkus et al. [46] compared the effect of sterilization on human cortical bone groups using acoustic emission (AE) analysis. The specimen used for experiments was compact tension specimen. The comparison was carried out using irradiated and non irradiated groups in both longitudinal and transverse direction. It was observed in experiments from the load displacement curves that the maximum force is lower for the irradiated groups than for the control groups for both crack growth directions. The fracture toughness was also lower for irradiated groups than non irradiated groups.

Vastel et al. [47] investigated different sterilization processing methods effect on the mechanical properties of human cancellous bone allografts of samples taken from femoral heads cadavers of 19–60 years of age. The irradiated and non irradiated samples were compared using

ultra sound wave propagation rate at a dose of 30 kGy. The results showed detoraition of 2.5% in the rate measured from non irradiated groups.

Dux et al. [48] examined the effects on yield and elastic properties after irradiation of bone specimens from bovine proximal tibiae. The results showed that there is no change in yield strain in irradiated specimens and non irradiated specimen. It was also determined that there is no variation in elastic modulus and the residual strain of irradiated specimens showed larger, bigger number of microfractures. Commonly used dosing 30kGy of sterilization does not varies elastic or yield properties of dense cancellous bone, but it causes modifications in damage processes, which results in increased permanent deformation.

Salehpour et al. [49] used gamma irradiation to find the effect on mechanical and material properties of collagen. The specimen was taken from goat patellar tendon bone. Each of the specimens was freezed and exposed to 40, 60 and 80 kGy of gamma irradiation. The specimens were tested in tension, and it has been found that at 40 kGy of radiation, maximum stresses and modulus was reduced by 37% and 8% respectively.

Anderson et al. [50] used cancellous bone taken from tibiae to find out stress at failure, strain at failure and elastic modulus irradiated at 10, 31, 51 and 60 kGy of gamma irradiation by compression test method. It has been determined at 60 kGy that no major variation in failure stress and normalized elastic modulus was found when these groups were compared with reference group.

Fidler et al. [51] studied the effect of gamma irradiation on bone of young human of patellar tendon allografts. These allografts were divided into four test groups, a control fresh frozen group and three fresh frozen irradiated groups. Three different doses of 20, 30, or 40 kGy of gamma irradiation were used. The test method used for specimens was tensile test method. The results were compared with fresh frozen control allografts and it has been found that the mechanical strength of fresh frozen allografts was reduced up to 15% at 20 kGy of irradiation. There was also considerable reduction in ultimate force, modulus, and ultimate stress at 20 kGy of radiation.

Curry et al. [52] studied the effect of ionizing radiation on allogeneic bone grafting sterilization. Specimens were taken from femora of four donors who received doses of 29.5 kGy,

94.7 kGy, or 17 kGy of ionizing radiation. The test results showed degradation in work to fracture but the young's modulus was unaffected by any level of radiation.

The literature survey reveals that different bones have been studied for the effect of X-rays or gamma radiations on bone properties. There are fewer studies on effect on gamma irradiation on hip joint bone of bovine's bones. Being a vital bone, the study of hip bone fracture behavior with gamma irradiation is essential for the treatment and modeling. Due to the research gap for the hip bone fracture behavior with effect of gamma irradiation, this study is focused on the categorization of mechanical properties variation of hip bone with effect of gamma irradiation. The following chapter describes the experimental set up for testing of the hip bone specimens after different dose of gamma irradiation.

Chapter 5

EXPERIMENTAL RESEARCH

This chapter describes the test technique used for the investigation of the effect of gamma irradiation. The chapter provides detail of test sample collection and preparation. The procedure of the tests is described in detail.

5.1. Fracture toughness testing

5.1.1. Test specimen

Bone test samples were taken from the hip bone of half calf male three year old bovine from local slaughter house. The test specimens were categorized into eight groups. Each group comprising of four specimens from three different bovine bones of same age i.e. three (3) years old. The bone was machined into 96 specimens using hack saw. Out of 96 samples, 48 specimens were prepared according to ASTM E-399 Standard [53] to measure fracture toughness. The final shape of specimen was obtained using file. Table 5.1 shows test matrix of machined test specimen for fracture toughness for longitudinal as well as transverse specimen. The geometry and location of the test specimen location on hip bone, fiber direction i.e. longitudinal or transverse direction is shown in Figure. 5.1, from where the test specimen is cut out from the bone. Figure 5.2 show the geometry of the test specimen. The specimens were painted with spackle pattern of white and black paint. In first step the specimen was painted with white paint with the help of spray and then it was sprayed with mist of black paint to obtain the black spackles. For the last color the distance of two (2) feet is necessary between spray and specimen [54-55].

The specimens were irradiated by insertion the bones in the vicinity of a radiation source cobalt 60 for a fixed time interval whereby the product is exposed to radiation emanating from the source. The irradiator was Ob-Servo IGNIS type Self Contained cobalt 60 dry storage irradiator of dimension 100×140.4×323.3 cm and 5 liters of volume capacity located at National Institute of Food & Agriculture (NIFA) in Peshawar. The maximum dose rate of the radiator was 10 kGy/h. Figure. 5.3 show the image of the irradiator. Different bones groups were stacked in the cylindrical vicinity column wise and were drawn after specific time for specific accumulated dose keeping gape of 25 kGy between two groups. The irradiator has a mechanism to move the

sample from the loading position to the irradiation position. The advantage of this irradiator is that they provide high dose rate and good dose uniformity that are essential for radiation research.

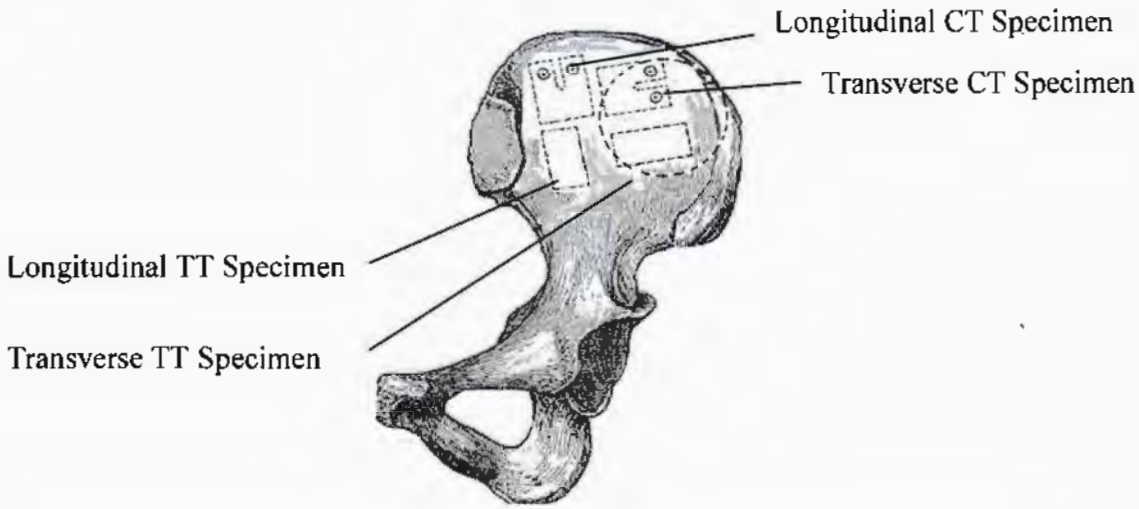

Figure 5.1: Hip joint bone & location of the CT and tensile test specimen.

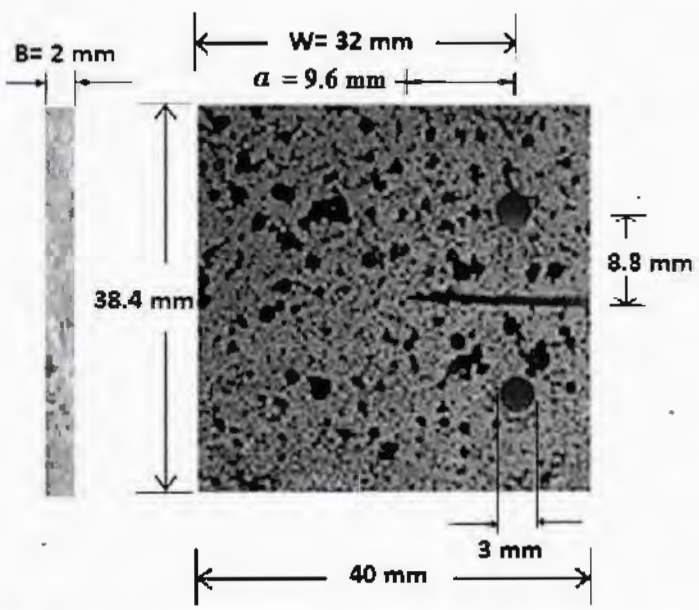

Figure 5.2: Compact tension specimen of hip joint bone.

Table 5.1: Test matrix of compact tension specimens

S.No.	Specimen Code	Dose (kGy)	LCT	TCT	Thickness(m)	Notch Length(m)	Width(m)
1	SP-1	0	✓	✓	0.002	0.0096	0.032
2	SP-2		✓	✓	0.002	0.0096	0.032
3	SP-3		✓	✓	0.002	0.0096	0.032
4	SP-4	25	✓	✓	0.002	0.0096	0.032
5	SP-5		✓	✓	0.002	0.0096	0.032
6	SP-6		✓	✓	0.002	0.0096	0.032
7	SP-7	50	✓	✓	0.002	0.0096	0.032
8	SP-8		✓	✓	0.002	0.0096	0.032
9	SP-9		✓	✓	0.002	0.0096	0.032
10	SP-10	75	✓	✓	0.002	0.0096	0.032
11	SP-11		✓	✓	0.002	0.0096	0.032
12	SP-12		✓	✓	0.002	0.0096	0.032
13	SP-13	100	✓	✓	0.002	0.0096	0.032
14	SP-14		✓	✓	0.002	0.0096	0.032
15	SP-15		✓	✓	0.002	0.0096	0.032
16	SP-16	125	✓	✓	0.002	0.0096	0.032
17	SP-17		✓	✓	0.002	0.0096	0.032
18	SP-18		✓	✓	0.002	0.0096	0.032
19	SP-19	150	✓	✓	0.002	0.0096	0.032
20	SP-20		✓	✓	0.002	0.0096	0.032
21	SP-21		✓	✓	0.002	0.0096	0.032
22	SP-22	175	✓	✓	0.002	0.0096	0.032
23	SP-23		✓	✓	0.002	0.0096	0.032
24	SP-24		✓	✓	0.002	0.0096	0.032

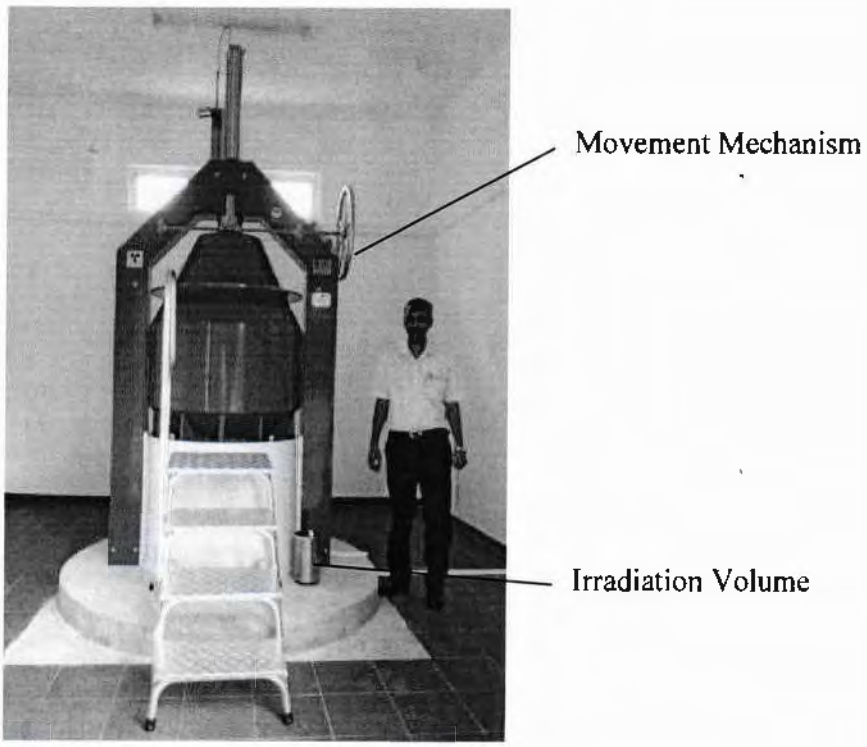

Figure 5.3: Ob Servo IGNIS type dry storage gamma irradiator of source cobalt 60.

5.1.2. Test procedure

The fracture toughness tests were performed using Universal testing machine, CMT 4304 in Pakistan Institute of Engineering and Applied sciences (PIEAS). The UTM have maximum load capacity of 30 kN with vertical test space (Displacement range) of +/-80 mm along. The UTM is connected with computer and camera setup as shown in Figure 5.4. The specimen was griped in loading clevis for the test. The clevis geometry is shown in the Figure 5.5. The test cross head speed of the machine was 0.5 mm/minute. During the test, the load and displacement was recorded. The crack tip of the CT specimen was observed using camera setup. The test was stopped as the crack started to grow.

5.1.3. Fracture toughness test data analysis

The fracture toughness K was calculated using the following equation [56].

$$K = \frac{P_C Y}{BW^{0.5}} \tag{5.1}$$

Where

$$Y = 29.6\left(\frac{a}{W}\right)^{0.5} - 185.5\left(\frac{a}{W}\right)^{1.5} + 655.7\left(\frac{a}{W}\right)^{2.5} - 1017\left(\frac{a}{W}\right)^{3.5} + 638.9\left(\frac{a}{W}\right)^{4.5} \quad (5.2)$$

In the above equation P_C is load, B is thickness, W is width and a is crack length.

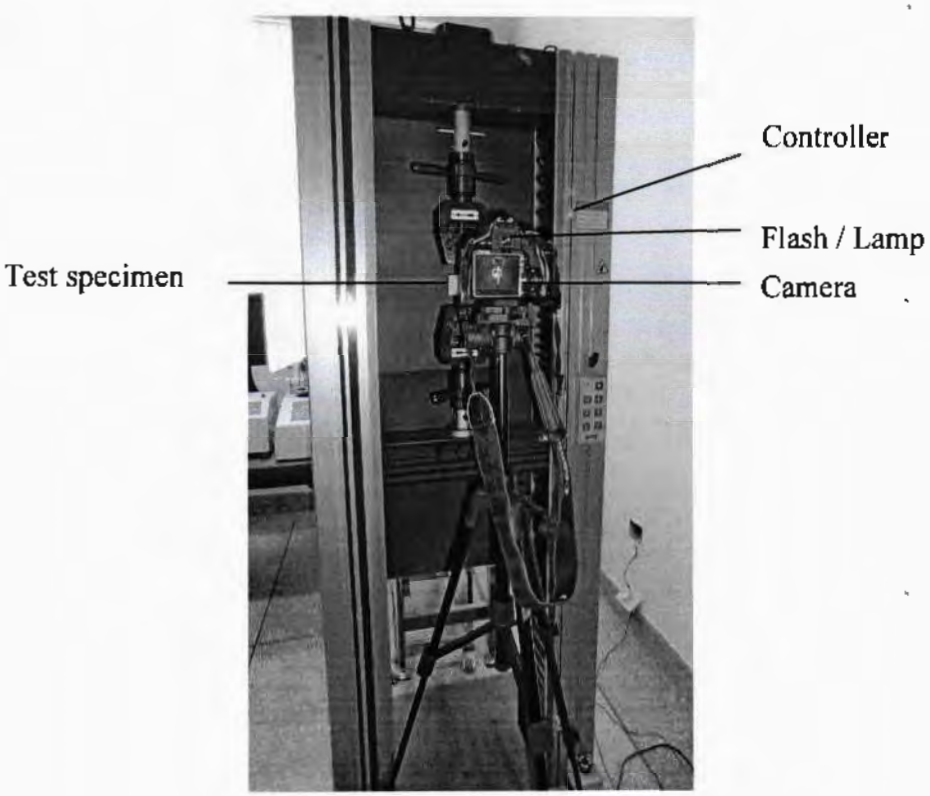

Figure 5.4: Universal testing machine with DIC Set Up.

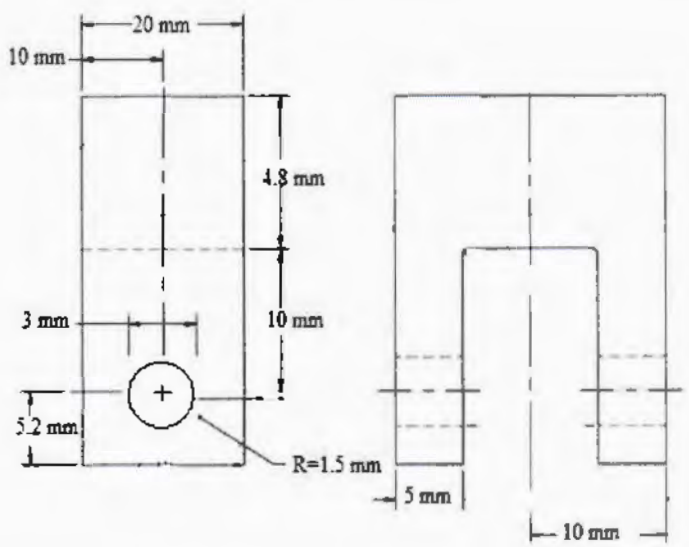

Figure 5.5: Compact tension testing clevis geometry.

5.1.4. DIC analysis of the CT specimens

The images of the crack tip were recorded by camera and computer setup shown in Figure 5.4. The images were numbered respectively. The images were processed using Vic-2D, DIC analysis software. The procedure is given in the following steps.

i) Starting software for analysis

Vic-2D software was started as shown in the Figure 5.6.

Figure 5.6: Vic-2D 2009 User interface

ii) Loading images

The images were loaded by clicking file menu then new then browsing folder and then selecting all images as shown in the Figure 5.7.

Figure 5.7: Loading images.

iii) Selecting reference image

By clicking right side of mouse the first image is selected as a reference image as encircled in Figure 5.8.

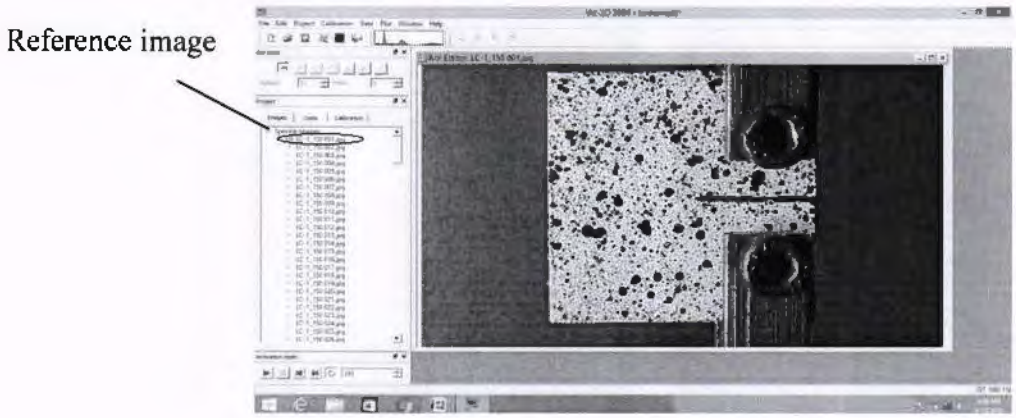

Figure 5.8: Reference image loading.

iv) Selecting area of interest

From the main menu of software interface the area of interest is selected as shown in Figure 5.9.

Figure 5.9: Area of interest selection.

v) Analyzing the images

By clicking analysis icon from Vic-2D user interface analysis window opens which shows run command to analyze the images shown in Figure 5.10, 5.11.

Figure 5.10: Preparation for analysis.

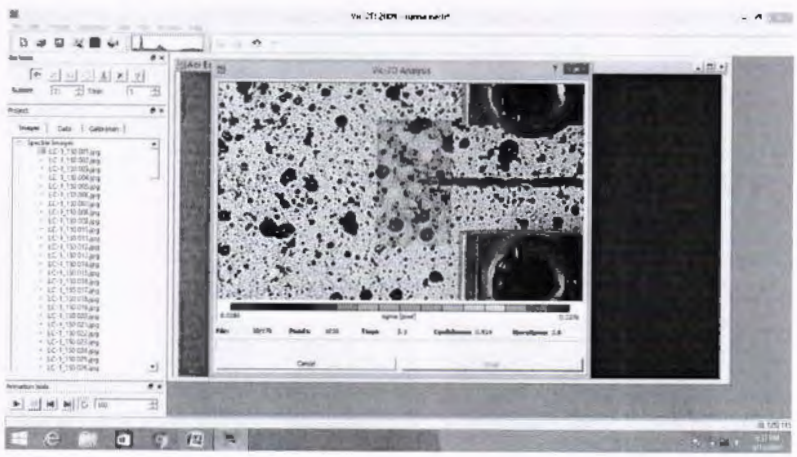

Figure 5.11: Running analysis.

vi) Strain calculation and plotting

From the Vic-2D user interface selecting the data tab and than from the post processing option the strain calculate tab is selected and the analysis started as shown in Figure 5.12, 5.13.

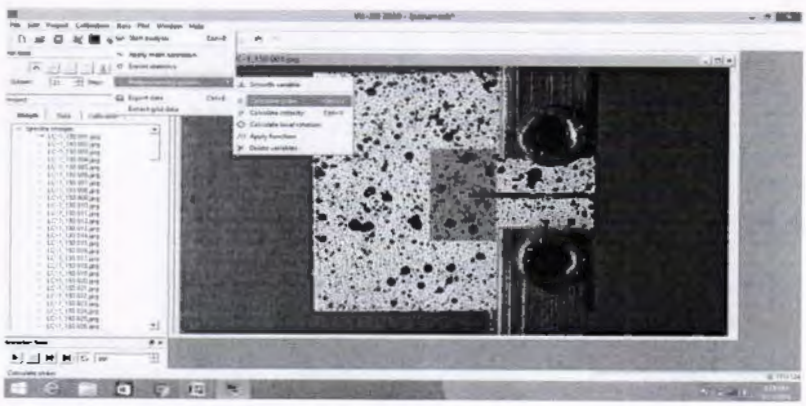

Figure 5.12: Strain calculation window after post processing.

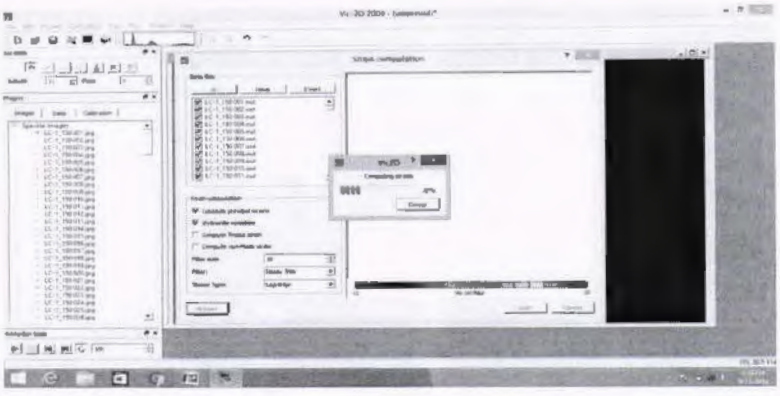

Figure 5.13: Strain calculation process.

vii) Completion of strain calculation

After strain processing the strain calculation is completed and the following windows open which shows the maximum strain at the crack tip along x-axis as shown in the Figure 5.14. By right click on the processed image strain along y-axis can also be determined as shown in Figure 5.15.

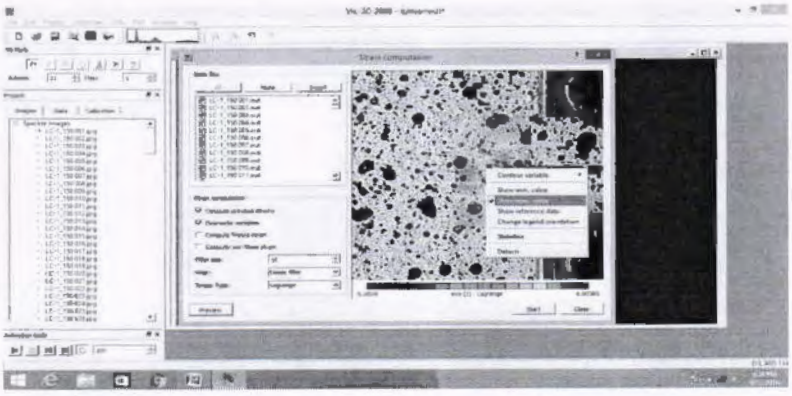

Figure 5.14: Maximum strain along x-axis.

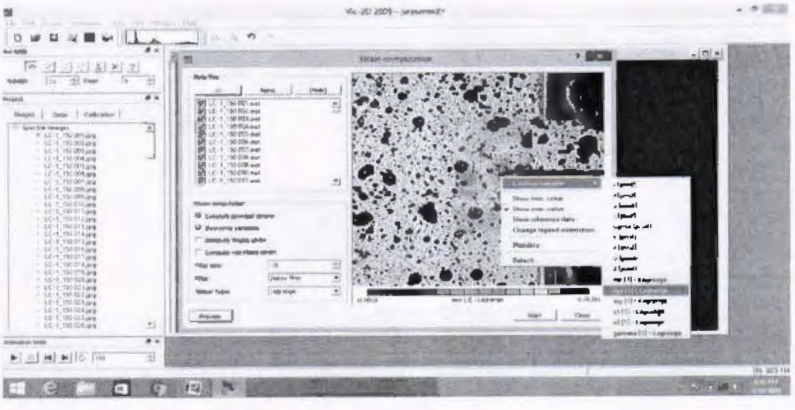

Figure 5.15: Maximum strain along y-axis.

5.2. Tensile testing

5.2.1. Test specimen

The specimen collection process was same as described in section 5.1.1. The specimens were prepared according to ASTM D 3039/D 3039M standard [57]. The tabs made of aluminum were bonded to the test specimen as shown in the Figure 5.16. The location of the tensile specimen on the hip joint bone is shown in Figure 5.1. The geometry of the specimen is shown in Figure 5.16. The irradiation process was same as described in section 5.1.1. Test matrix for longitudinal and transverse tensile specimens is given in Table 5.2 and Table 5.3 respectively.

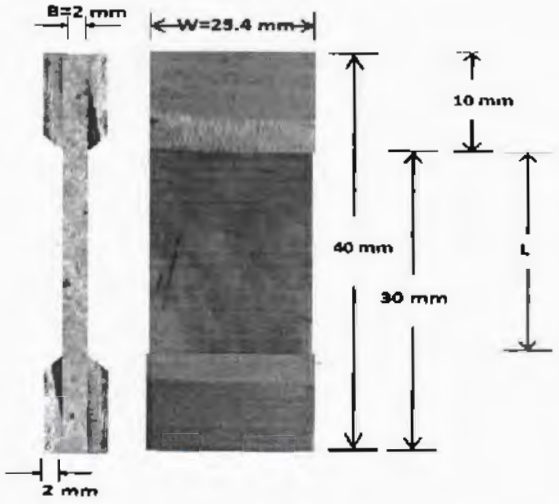

Figure 5.16: Tensile test specimen

Table 5.2: Test matrix of longitudinal tensile test specimens.

S.No.	Specimen Code	Dose (kGy)	LT	Width (m)	Thickness (m)	Original Length (m)
1	LT-1	0	✓	0.0254	0.002	0.02
2	LT-2		✓	0.0254	0.002	0.02
3	LT-3		✓	0.0254	0.002	0.02
4	LT-4	25	✓	0.0254	0.002	0.02
5	LT-5		✓	0.0254	0.002	0.02
6	LT-6		✓	0.0254	0.002	0.02
7	LT-7	50	✓	0.0254	0.002	0.02
8	LT-9		✓	0.0254	0.002	0.02
9	LT-11	75	✓	0.0254	0.002	0.02
10	LT-12		✓	0.0254	0.002	0.02
11	LT-14	100	✓	0.0254	0.002	0.02

12	LT-15		✓	0.0254	0.002	0.02
13	LT-16	125	✓	0.0254	0.002	0.02
14	LT-17		✓	0.0254	0.002	0.02
15	LT-19	150	✓	0.0254	0.002	0.02
16	LT-21		✓	0.0254	0.002	0.02
17	LT-22	175	✓	0.0254	0.002	0.02
18	LT-24		✓	0.0254	0.002	0.02

Table 5.3: Test matrix of transverse tensile test specimens.

S.No.	Specimen Code	Dose (kGy)	TT	Width (m)	Thickness (m)	Original Length (m)
1	TT-1	0	✓	0.0254	0.002	0.02
2	TT-3		✓	0.0254	0.002	0.02
3	TT-5	25	✓	0.0254	0.002	0.02
4	TT-6		✓	0.0254	0.002	0.02
5	TT-7	50	✓	0.0254	0.002	0.02
6	TT-8		✓	0.0254	0.002	0.02
7	TT-10	75	✓	0.0254	0.002	0.02
8	TT-15	100	✓	0.0254	0.002	0.02
9	TT-16	125	✓	0.0254	0.002	0.02
10	TT-20	150	✓	0.0254	0.002	0.02
11	TT-21		✓	0.0254	0.002	0.02
12	TT-24	175	✓	0.0254	0.002	0.02

5.2.2. Test procedure and data analysis

The specimens were tested in same UTM as described in section 5.1.2. The specimen was gripped in the machine as shown in Figure 5.17. The test was performed at a cross head speed of 0.5 mm/minute. During the test the applied load and the displacement were recorded by PC. The test was stopped after specimen failure.

The strength of the specimen was calculated using the following equation.

$$\sigma = \frac{F}{A} \tag{5.3}$$

Where F is the force at specimen failure and A is the cross sectional area of the specimen. The strain at failure was calculated using the following equation.

$$\varepsilon = \frac{\delta}{l} \tag{5.4}$$

Where δ is change in length and l is gauge length. The young modulus was calculated using following equation.

$$E = \frac{\sigma_{max}}{\varepsilon_{max}} \tag{5.5}$$

Where σ_{max} is stress and ε_{max} is strain of the specimen

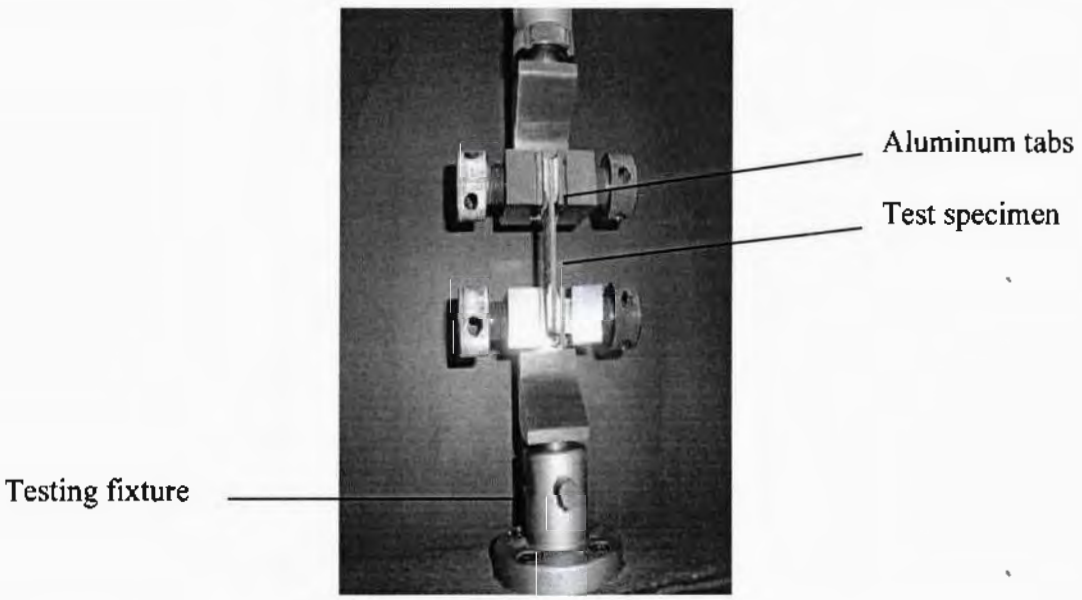

Figure 5.17: UTM with tensile test specimen setup.

The test results of the fracture toughness and tensile experiments are presented and discussed in the next chapter.

Chapter 6

EXPERIMENTAL RESULTS

This chapter presents the experimental results of the current research. The chapter presents results of fracture toughness variation with gamma radiation dose. In this chapter variation in young modulus and ultimate strength of the hip joint bone specimen is also presented. The DIC results are presented in the last section of the chapter.

6.1. Effect of gamma radiation on fracture toughness

The fracture toughness variation with gamma dose for longitudinal specimen is shown in Figure 6.1. The fracture toughness decreases with gamma dose. The maximum and minimum value of fracture toughness is 2.6E+06 & 3.3E+04 Nm-3/2 respectively. The percentage difference in fracture toughness is 13%, 28%, 32%, 51%, 66%, 81%, and 98% respectively for dose range of 25 kGy to 175 kGy. The error bar sizes show that variation among different samples is slight.

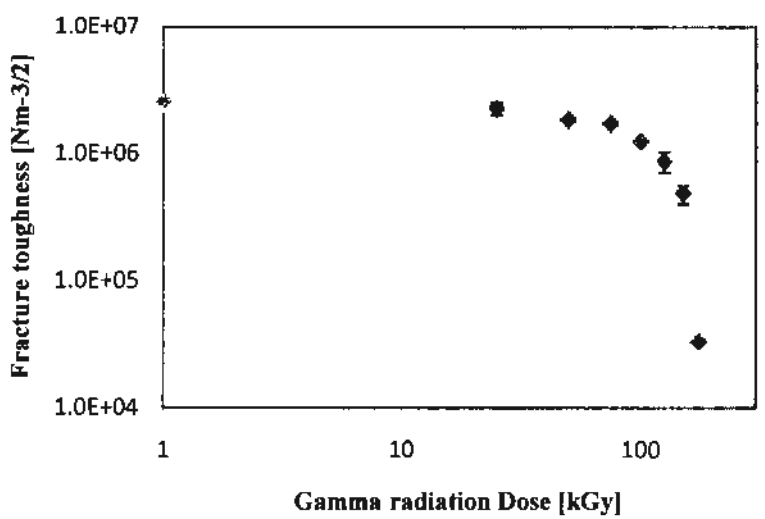

Figure 6.1: Fracture toughness versus gamma radiation dose for longitudinal specimen.

The effect of gamma radiation on fracture toughness on transverse specimen of hip bone is shown in Figure 6.2. The figure shows that the fracture toughness decreases as the gamma radiation dose increases. The maximum and minimum value of fracture toughness is 4.3E+06 & 1.9E+05 Nm-3/2 respectively. The fracture toughness decrease is steeper up to 50 kGy. The

reduction of the fracture toughness is slight between 50 kGy and 100 kGy. The percentage difference in fracture toughness is 84%, 92% and 96 % respectively for the gamma radiation dose range of 125 kGy to175 kGy. The error bar sizes show that variation among different samples is slight.

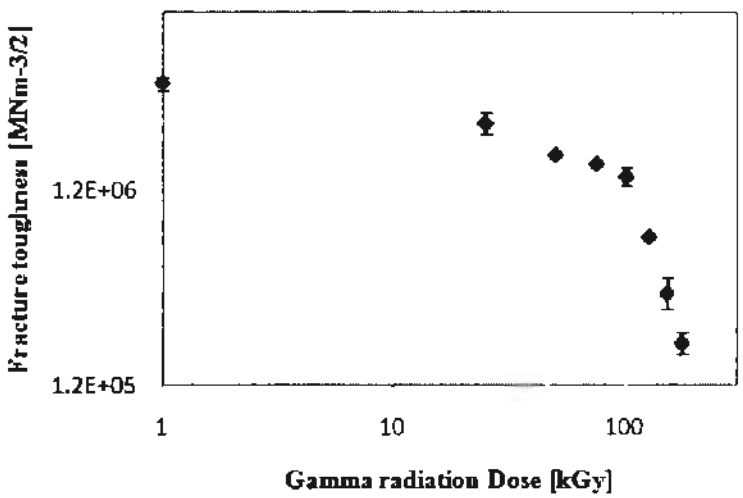

Figure 6.2: Fracture toughness versus gamma radiation dose for transverse specimen.

The values of fracture toughness in the longitudinal direction are generally lower than those in the transverse direction. This is due to the presence of the cement lines in the microstructure. These are narrow regions around the outermost lamellae in the osteons, and they usually form the weakest component of bone. Crack propagation parallel to the osteons can occur much more easily through these regions and thus decreases the fracture toughness in the longitudinal direction. When a crack is propagating perpendicular to an osteon its direction is changes whenever it reaches a cement line, thus resulting in blunting of the crack.

Figure 6.3 and Figure 6.4 illustrate images of compact tension specimen for longitudinal and transverse specimen respectively. Figure 6.3 shows that crack path is parallel to the osteons, thus facing least resistant. Figure 6.4 shows the transverse CT specimen fracture. The crack path is perpendicular to the osteons and so the resistance is higher in this case resulting in higher fracture toughness values.

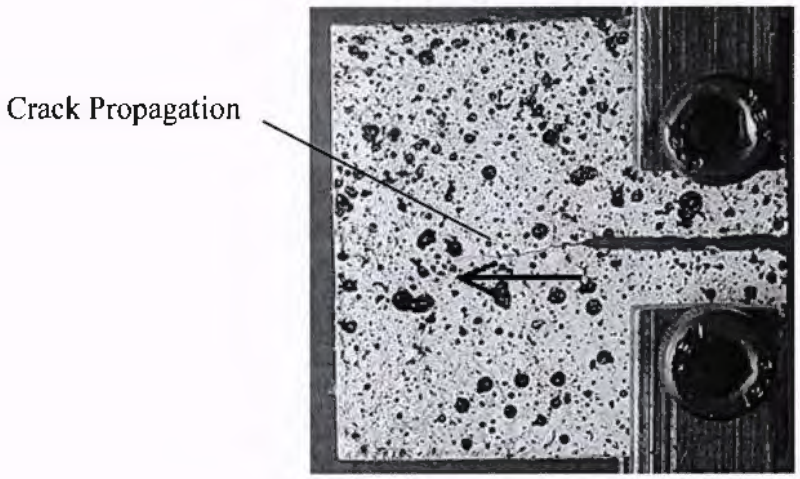

Figure 6.3: Longitudenal compact tension specimen after failure.

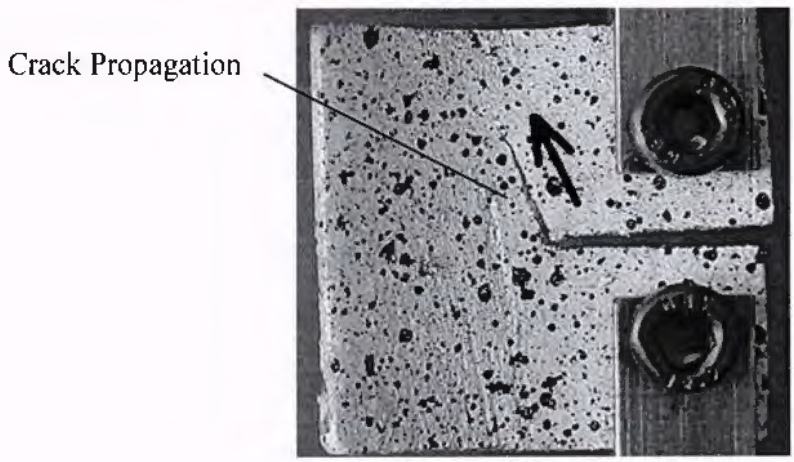

Figure 6.4: Transverse compact tension specimen after failure.

6.2. Effect of gamma radiation on modulus of elasticity

The effect of gamma irradiation on the young modulus of the bovine hip bone is shown in Figure 6.5. The figure shows overall decrease for longitudinal direction. The maximum and minimum value of modulus of elasticity is 4.6E+09 & 1.4E+07 N/m^2 respectively. The decrease of young modulus is steeper for all dose of gamma radiation. The figure illustrates that the young modulus for longitudinal CT specimen is less than in transverse specimen. The modulus of elasticity for longitudinal specimen reduces by 61%, 93%, 95%, 96%, 97%, 98% and 99% respectively for dose range of 25 kGy to 175 kGy.

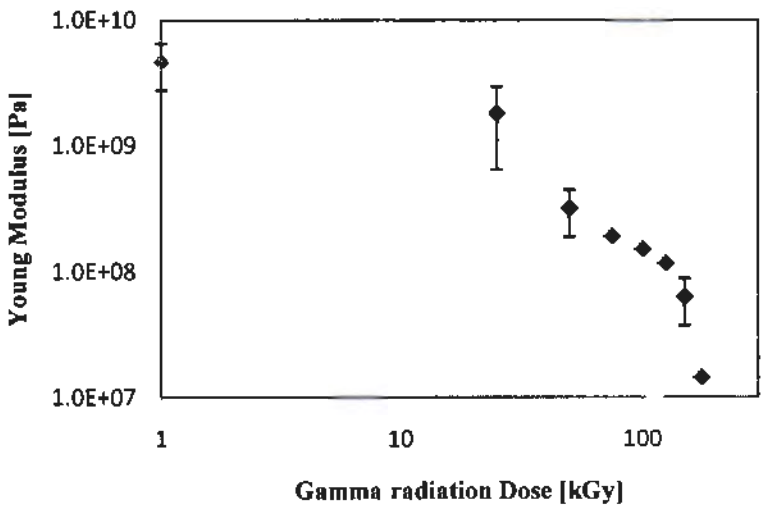

Figure 6.5: Young modulus versus gamma radiation dose for longitudinal specimen.

The young modulus variation with gamma radiation doses for transverse specimen is shown in the Figure 6.6. The figure shows overall decrease in young modulus with gamma irradiation. The maximum and minimum value of modulus of elasticity is 1.4E+10 & 1.5E+07 N/m^2 respectively. The young modulus is steeper for all doses of gamma radiation and it is more than for longitudinal compact specimen. The modulus of elasticity is reduces by 78%, 92%, 95%, 97%, 98%, 99%, and 100% respectively for the dose range of 25 kGy to 175. The error bar sizes show that variation among different samples is slight.

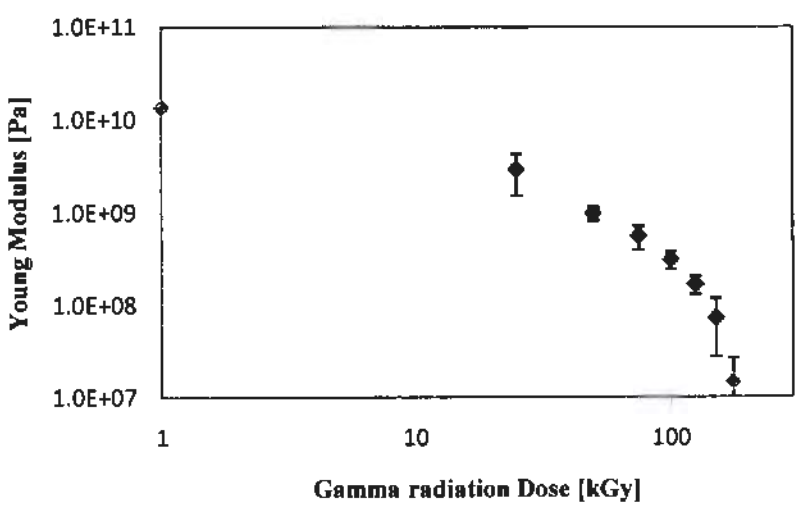

Figure 6.6: Young modulus versus gamma radiation dose for transverse specimen.

6.3. Effect of gamma radiation on ultimate strength

The variation of ultimate strength with different doses of gamma radiation on longitudinal specimen is shown in the Figure 6.7. The figure shows that the reduction is steeper from 0-50 kGy. The maximum and minimum value of ultimate strength is 2.1E+07 & 2.8E+06 N/m² respectively. The percentage difference in ultimate strength for longitudinal specimen is 68 %, 74 %, 79 % 85 % and 86% respectively for dose range of 75 kGy to 175 kGy.

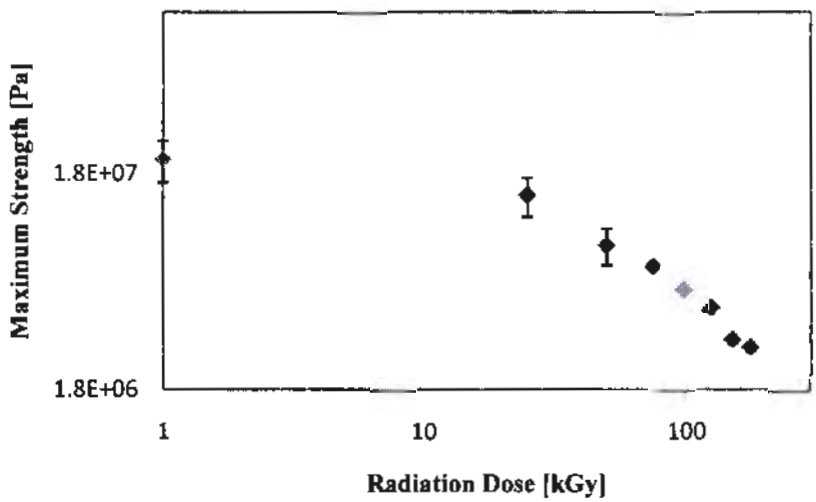

Figure 6.7: Ultimate strength versus gamma radiation dose for longitudinal specimen.

The effect of gamma irradiation on the Ultimate strength on transverse specimens is shown in the Figure 6.8. The figure shows steeper decrease for doses 0 kGy to 50 kGy. The maximum and minimum value of ultimate strength is 4.6E+07 & 2.7E+06 N/m² respectively. The percentage difference in ultimate strength for transverse compact tension specimen is 59 % and 70 % for 75 kGy and 100 kGy of gamma doses respectively. The reduction of the ultimate strength is slight for the dose range of 125 kGy and 175 kGy.

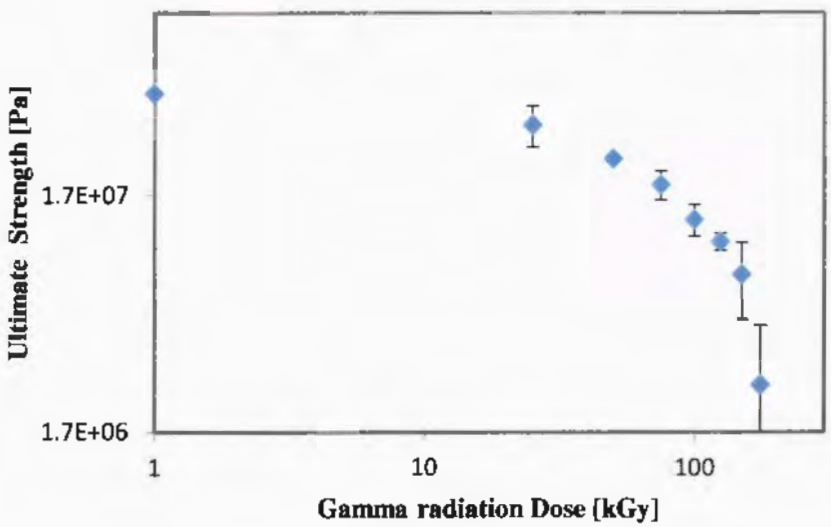

Figure 6.8: Ultimate strength versus gamma radiation dose for transverse specimen.

6.4. DIC analysis results

The procedure of DIC analysis for calculating strain field around crack tip of CT specimens using DIC analysis was described in section 5.1.4 of the previous chapter. In this section the results of DIC analysis are presented. The DIC analysis results are summarized Table 6.1 and 6.2 for longitudinal and transverse CT specimen respectively. The table lists the radiation dose values, load level and strain values i.e, e_{xx}, e_{yy}, e_1 and e_2. The corresponding DIC images of the specimens at specified load and dose values are also shown in the figure next to each strain values.

Table 6.1: Maximum strain field of CT longitudinal specimen.

Radiation Dose (kGy)	Specimen Code	Maximum Load (N)	e_{xx}	e_{yy}	e_1	e_2
0	SP-1	89.8564	0.023 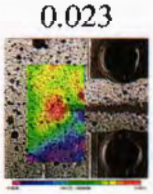	0.0535 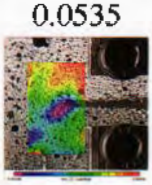	0.045 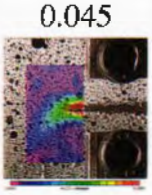	0.0197 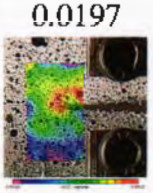

	SP-2	88.38958	0.0185 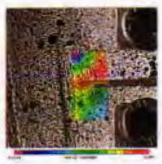	0.0462 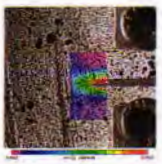	0.046 	0.016 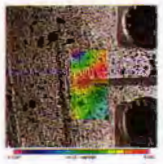
	SP-3	87.71	0.0123 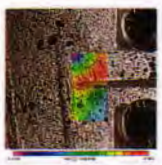	0.045 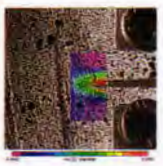	0.0428 	0.00185 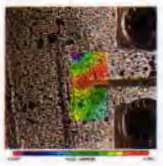
25	SP-4	86.2431	0.0083 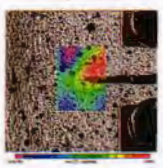	0.0446 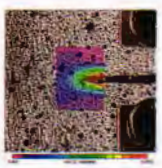	0.0445 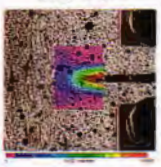	0.0081 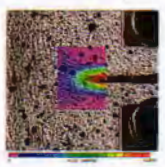
	SP-5	77.9355	0.0081 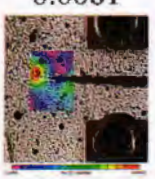	0.0402 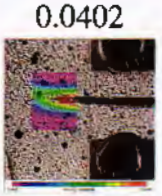	0.0402 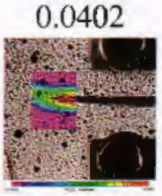	0.0079 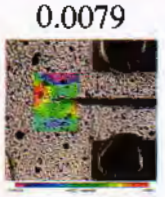
	SP-6	68.7632	0.0067 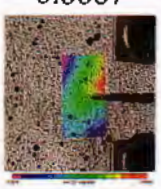	0.0372 	0.0372 	0.00404 
50	SP-7	65.9374	0.00635 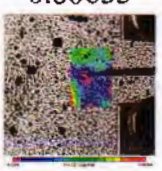	0.0372 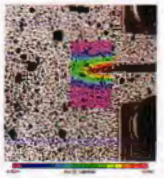	0.0401 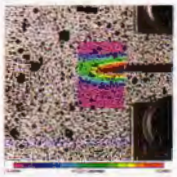	0.0051 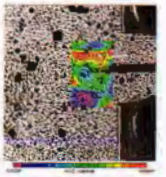
	SP-8	63.6829	0.0056 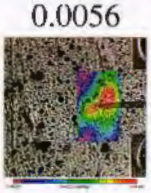	0.0366 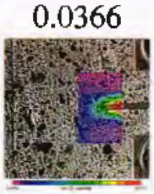	0.0372 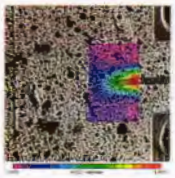	0.0043 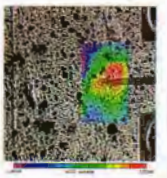

	SP-9	61.6446	0.0053 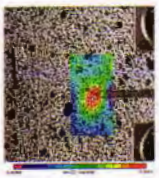	0.0324 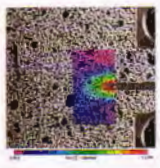	0.0324 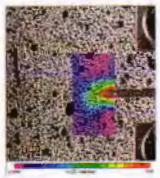	0.00525 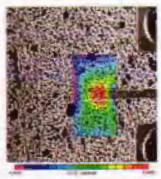
75	SP-11	59.4022	0.004 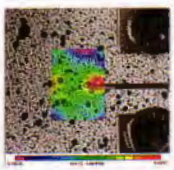	0.0304 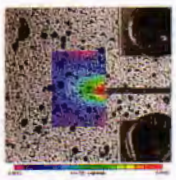	0.0302 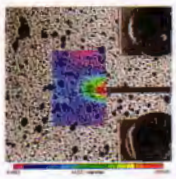	0.0037 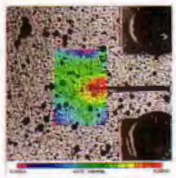
	SP-12	57.4953	0.00366 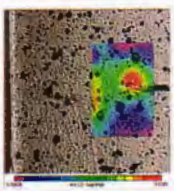	0.0296 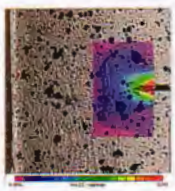	0.0297 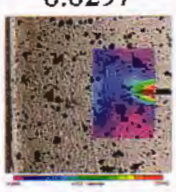	0.00264 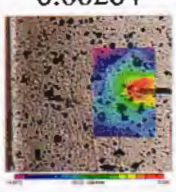
100	SP-13	45.4333	0.00316 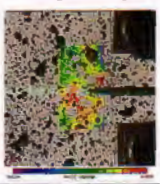	0.0231 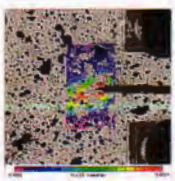	0.0217 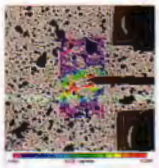	0.00312 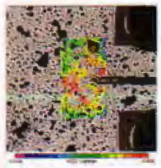
	SP-14	42.9512	0.0029 	0.0181 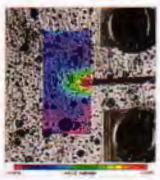	0.0181 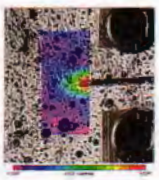	0.0029 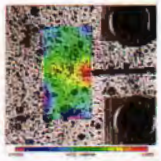
	SP-15	40.3633	0.00268 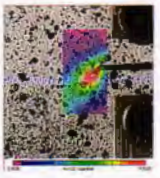	0.015 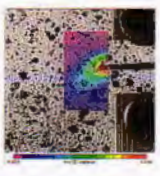	0.0148 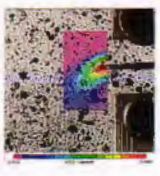	0.00204 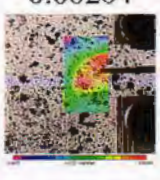
125	SP-16	33.9614	0.00186 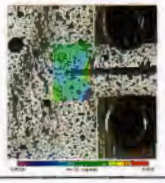	0.0147 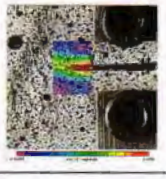	0.0147 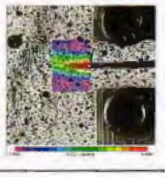	0.00185 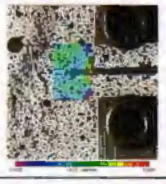

	SP-17	32.1453	0.00178 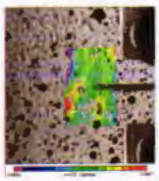	0.0143 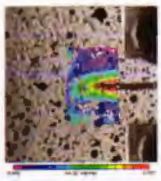	0.0143 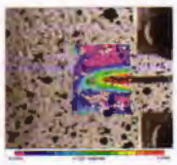	0.00166 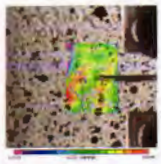
150	SP-19	19.1298	0.0011 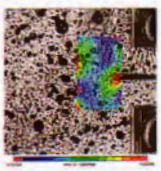	0.0096 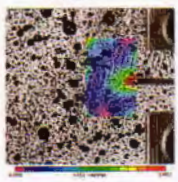	0.0097 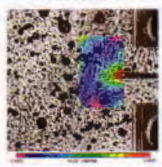	0.0076 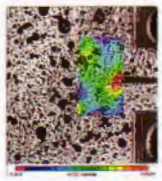
	SP-20	17.2077	0.001 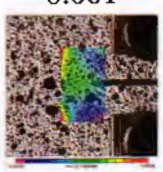	0.00675 	0.00675 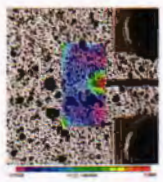	0.001 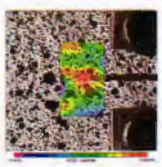
	SP-21	13.6814	0.001 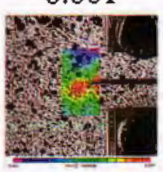	0.00525 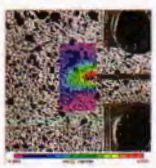	0.00521 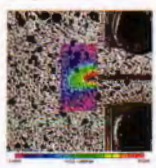	0.001 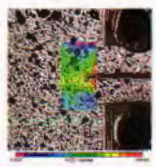
175	SP-22	1.1351	0.0005 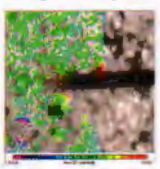	0.00056 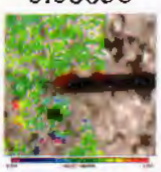	0.000391 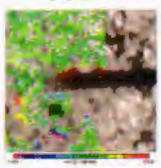	0.0002 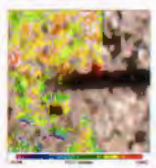

Table 6.2: Maximum strain field of CT transverse specimen.

Radiation Dose (kGy)	**Specimen Code**	**Maximum Load (N)**	e_{xx}	e_{yy}	e_1	e_2
0	SP-2	155.4809	0.011 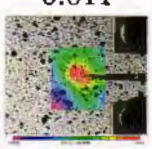	0.063 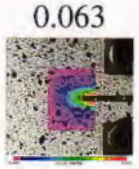	0.063 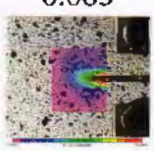	0.0084 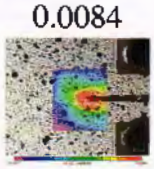

	SP-3	139.0452	0.01055 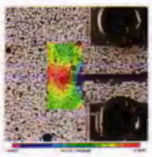	0.0565 	0.0564 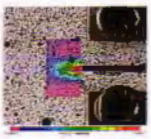	0.0087 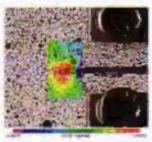
25	SP-4	104.0474	0.0099 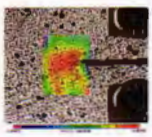	0.0426 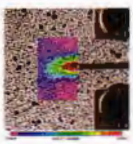	0.0426 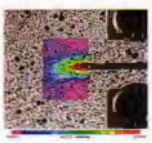	0.0097 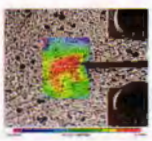
	SP-5	94.0565	0.0098 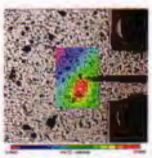	0.0414 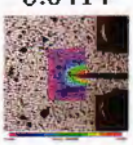	0.0421 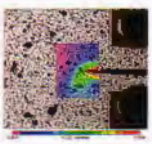	0.00335 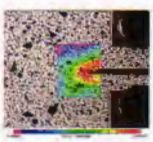
	SP-6	80.6687	0.0097 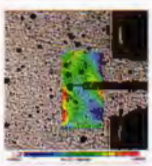	0.0324 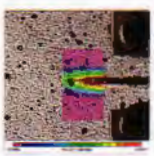	0.0324 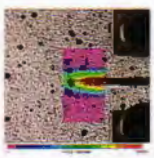	0.0089 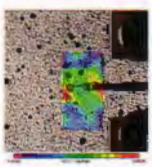
50	SP-7	64.3777	0.00735 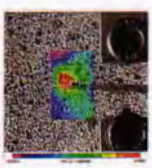	0.0308 	0.0300 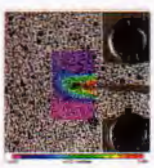	0.00710 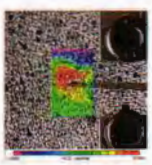
	SP-8	64.177	0.0053 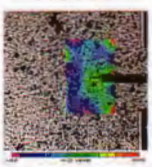	0.026 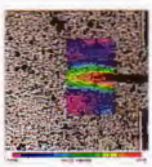	0.025 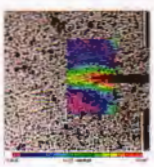	0.0048 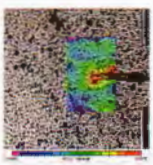
	SP-9	61.5365	0.0048 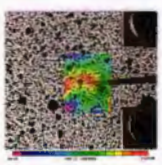	0.026 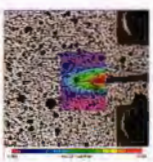	0.026 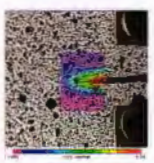	0.00389 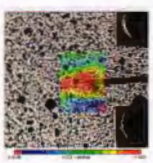

75	SP-10	60.2703	0.00416 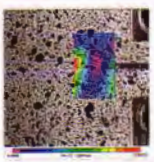	0.0248 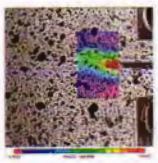	0.0236 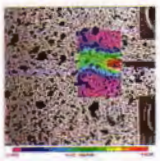	0.004 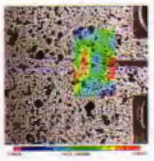
	SP-11	56.3451	0.0041 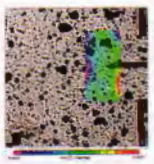	0.0237 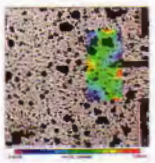	0.0236 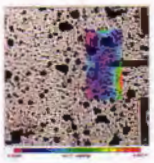	0.0036 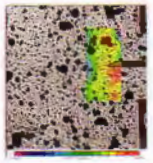
	SP-12	55.8608	0.00385 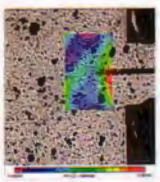	0.0232 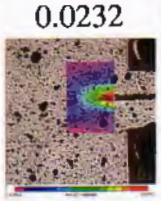	0.0232 	0.00378 
100	SP-13	54.2414	0.00368 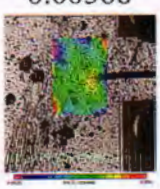	0.023 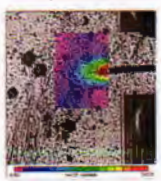	0.0213 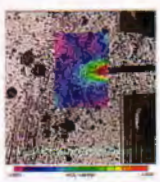	0.003 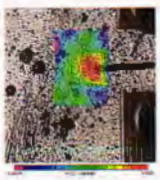
	SP-14	49.6406	0.00365 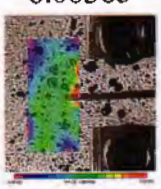	0.0208 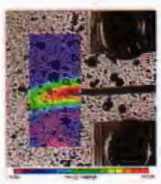	0.0205 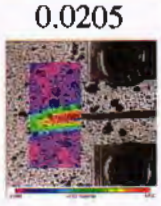	0.00315 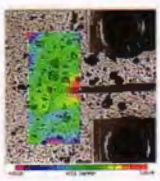
	SP-15	43.4355	0.0034 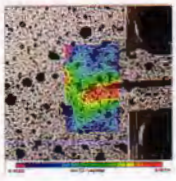	0.0196 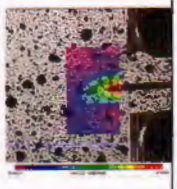	0.0203 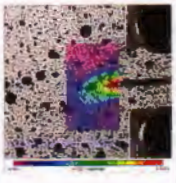	0.00246 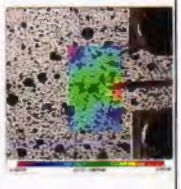
125	SP-16	24.6841	0.00295 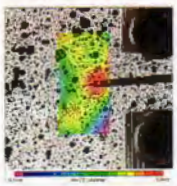	0.0192 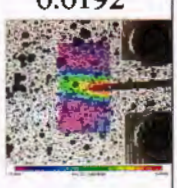	0.0192 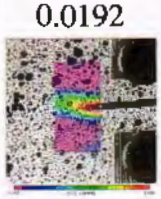	0.0029 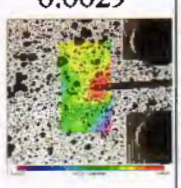

	SP-17	24.109	0.0028 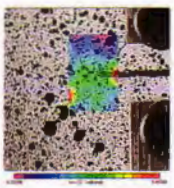	0.018 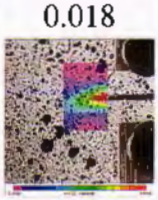	0.018 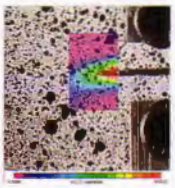	0.0028 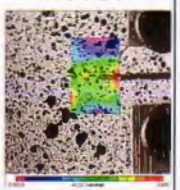
	SP-18	23.4279	0.00248 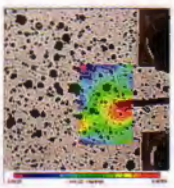	0.0151 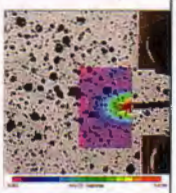	0.0151 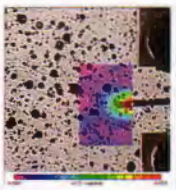	0.0022 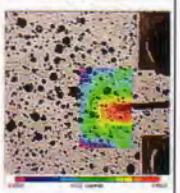
150	SP-19	15.0133	0.00385 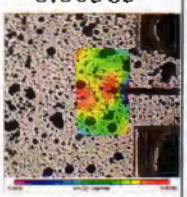	0.0133 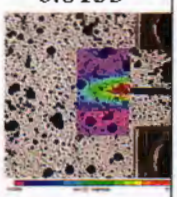	0.0133 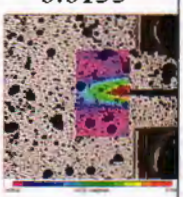	0.00355 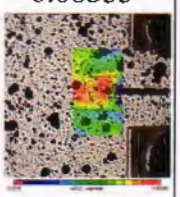
	SP-20	12.2437	0.00232 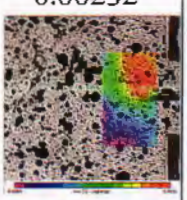	0.0119 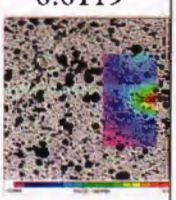	0.0119 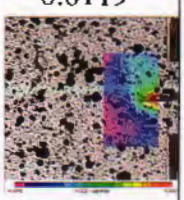	0.00206 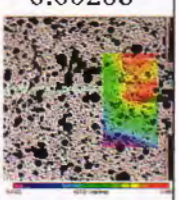
	SP-21	9.8524	0.0019 	0.0103 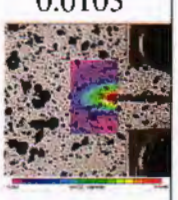	0.0101 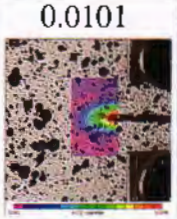	0.0014 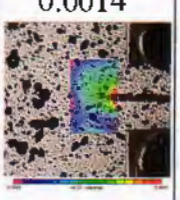
175	SP-22	2.1945	0.0016 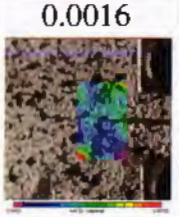	0.0079 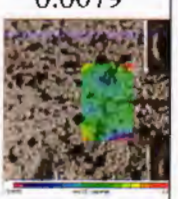	0.0088 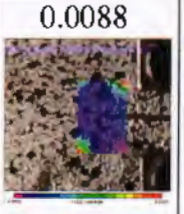	0.00148 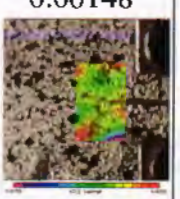

	SP-24	1.9977	0.00064 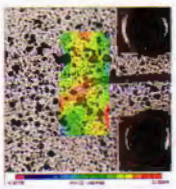	0.00091 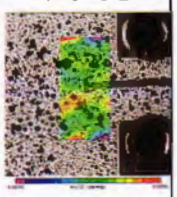	0.00125 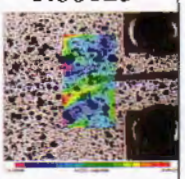	0.00061 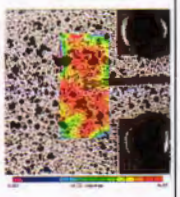

Figure 6.9 and 6.10 plot strain e_{xx} and e_{yy} against radiation dose for longitudinal and transverse specimens respectively. The strain values are more for e_{yy} than e_{xx} for both longitudinal and transverse specimen.

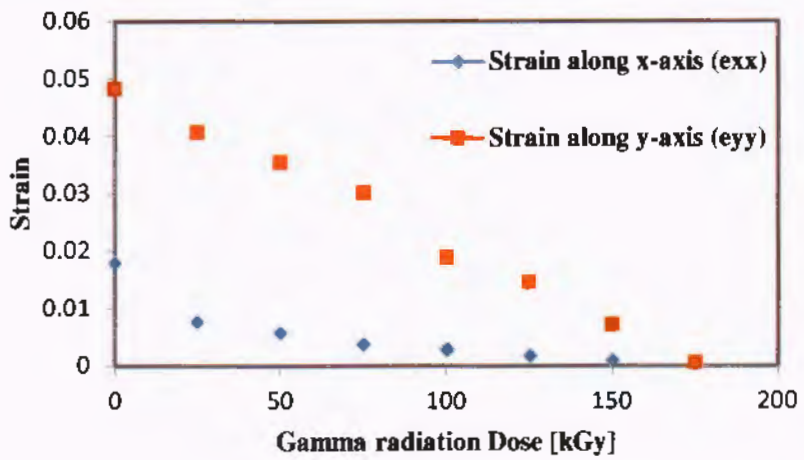

Figure 6.9: Strain along x-axis, y-axis versus gamma radiation for longitudinal CT specimen.

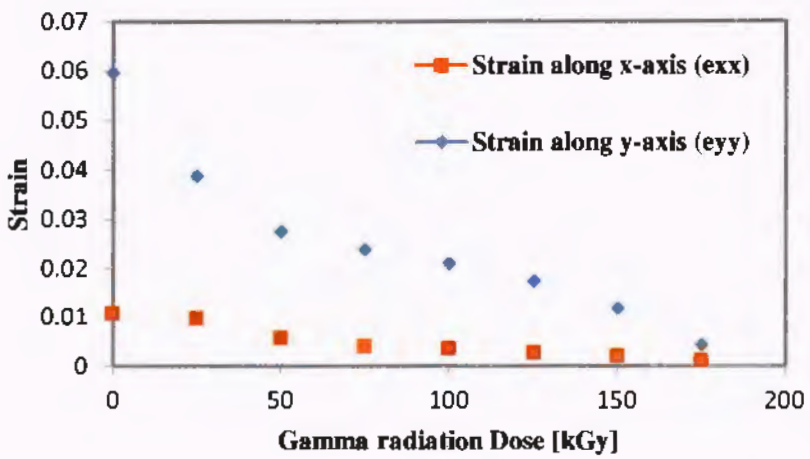

Figure 6.10: Strain along x-axis, y-axis versus gamma radiation for transverse CT specimen

There is sharp decrease in e_{yy} but for e_{xx} the decrease is slow with respect to gamma irradiation. The trend of variation for both longitudinal and transverse specimens is same and at 175 kGy the strain is nearly equal to zero for both types of specimen.

6.5. Discussion of the test results

The trend of the variation of fracture toughness, young modulus and ultimate strength of longitudinal specimen was evaluated by fittings curves to the experimental data. The trend can be best represented by fitting exponential function to the data as shown in Figure 6.11. The fracture toughness, young modulus and ultimate strength decease exponentially with gamma radiation dose.

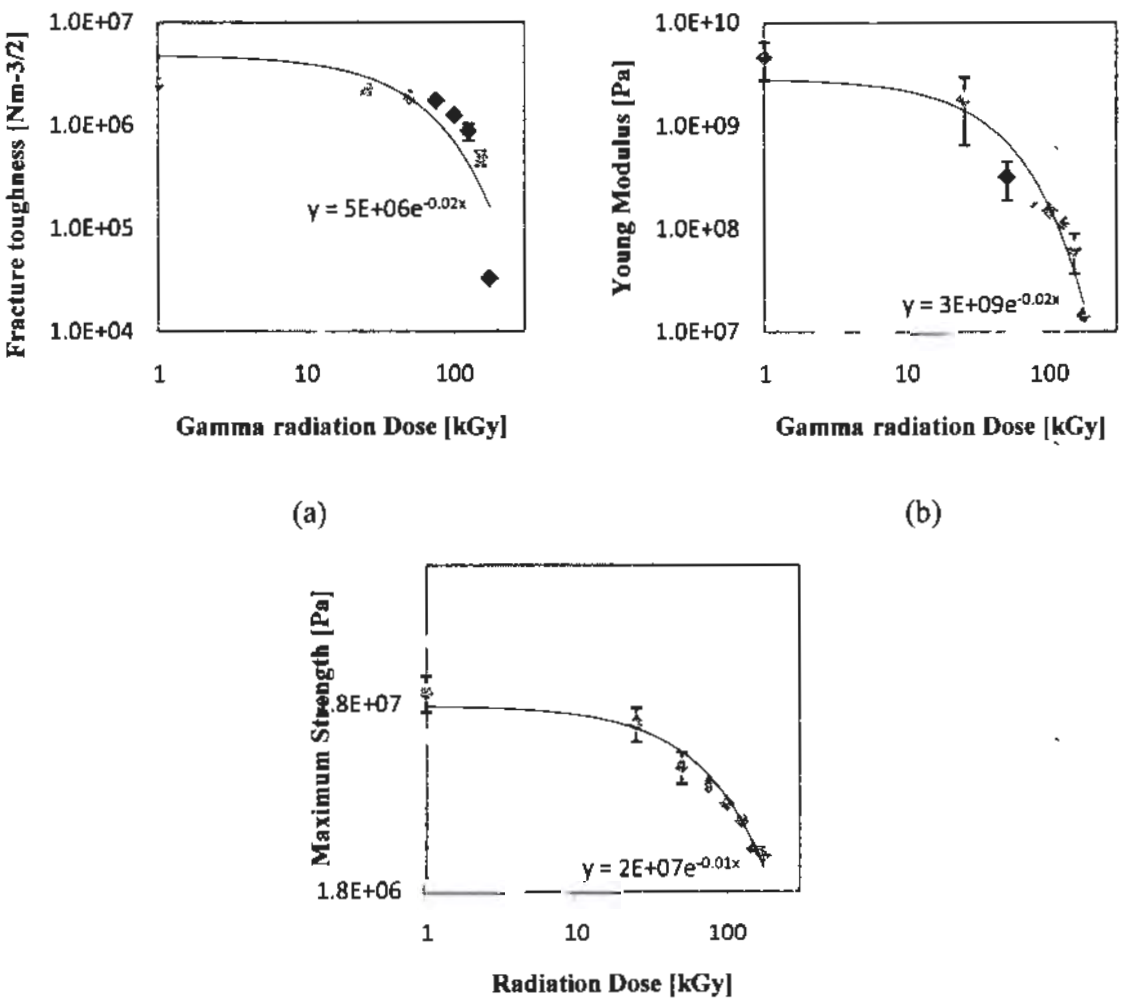

Figure 6.11: Trend line fitting of (a) Fracture toughness, (b) Young modulus and (c) Ultimate strength versus gamma radiation dose for longitudinal specimens.

The Figure 6.11 shows that the young modulus variation is more sensitive to gamma radiation dose than that of fracture toughness and ultimate strength. The variation in the fracture toughness is moderate and the variation is severe for ultimate strength to gamma radiation.

For transverse specimen the trend of variation of fracture toughness, young modulus and ultimate strength can be also represented by exponential function as shown in Figure 6.12. The figure shows that the young modulus variation is more sensitive to gamma radiation dose than that of fracture toughness and ultimate strength. The variation in the fracture toughness is moderate and the variation is severe for ultimate strength.

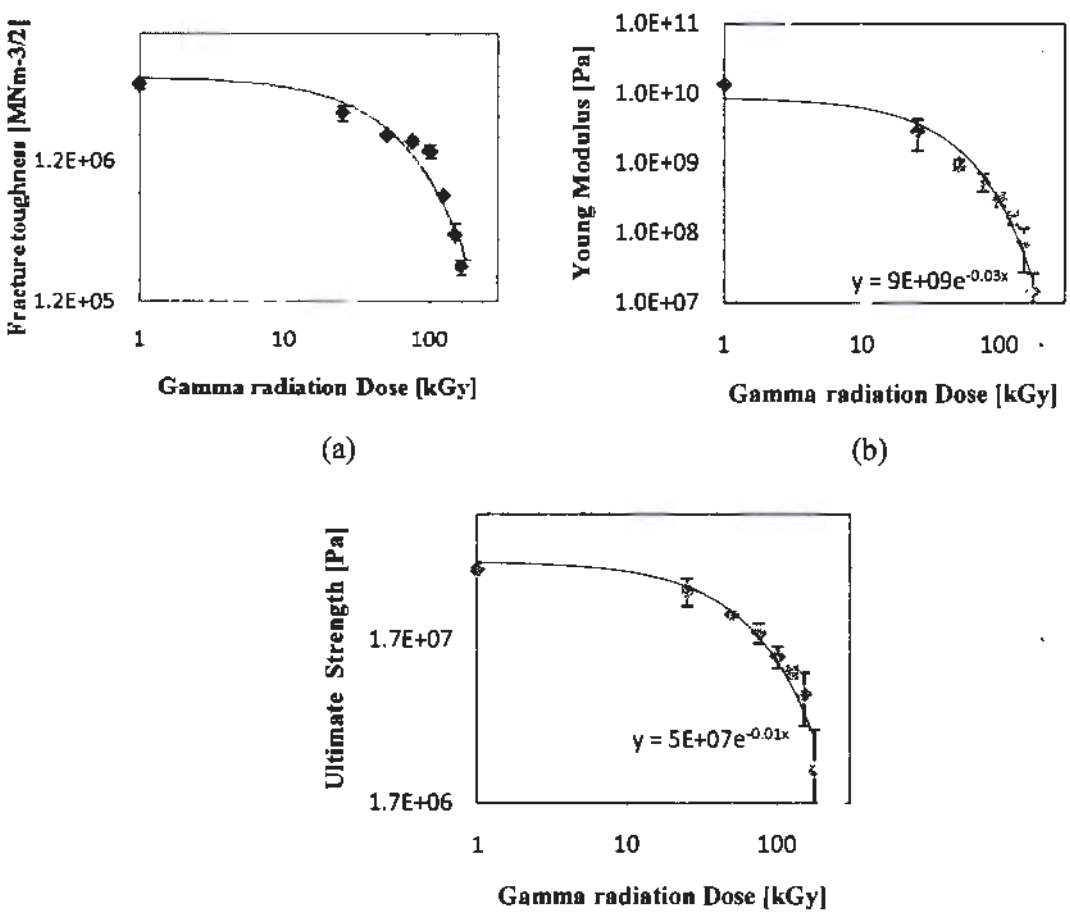

Figure 6.12: Trend line fitting of (a) Fracture toughness, (b) Young modulus and (c) Ultimate strength versus gamma radiation dose for transverse specimens.

Comparing results with literature, a small dose response reduction was observed to ultimate stress up to 23 kGy, but a large decrease was observed at 60 kGy [58]. Similar trends have been observed from bone tendon bone allografts in which the maximum stress decreased by 37% for those irradiated at 40 kGy, 68% at 60 kGy and 76% at 80 kGy [49], whereas lower doses of 20 and 30 kGy reduced the ultimate strength by 11–27% [43, 59]. Increasing the gamma dose with numerous small increments shows that this relationship is non linear with a dose of 27 kGy causing a reduction in strength of 20%, but a dose of 37 kGy causing a reduction of 65% [60].

Comparing test results with Barth [37] there is severe degradation of ductility fracture toughness and strength at high dose of 630 kGy for human cortical bone. Russell et al. [39] reported similar behavior of results of degradation of fracture toughness and mechanical properties for a dose of 25 kGy for bovine cortical bone. Balsly [45] use two allograft and conventional testing method for testing and it was found that there are no changes in modulus of elasticity but the strength decrease for one allograft and vice versa for second graft.

Similarly Burton et al. [41] studied the cortical bone at 33 kGy and used three point bending testing. It was reported that there is a decrease in the ultimate stress and work of fracture as similar to the current research. The initial mechanical properties were also analyzed by Gibbons et al. [43] with optical strain analysis on goat patellar tendon bone and it was reported that there is no effect on other mechanical properties but the ultimate stress is decreases after 30 kGy of dose.

Tu¨fekci [44] used 30 kGy of dose and found decrease of 9% in ultimate strength which is in our case is same in both longitudinal as well as in transverse direction. The results of fracture toughness and modulus of elasticity are different in the previous and current research. The results of Vastel et al. [47] also are similar with current research at 30 kGy of dose. Also the study of Salehpour et al. [49] have similar results for ultimate stress and modulus of elasticity with different dose range.

Chapter 7

CONCLUSIONS AND FUTURE RECOMMENDATIONS

In this thesis the effect of gamma irradiation on fracture toughness, strength and young modulus of bovine's hip bone specimens has been investigated. Fracture toughness was tested using CT specimens; tensile strength and young modulus were tested using flat specimens. Specimens were irradiated from 0 kGy to 175 kGy. The strain fields at the crack tip of CT specimens were examined using digital image correlation technique. The conclusions of the research are summarized in section 7.1 and future recommendations are presented in section 7.2 respectively.

7.1. Conclusions

- The fracture toughness, young modulus and strength were observed to be decreased due to gamma irradiation.
- The trend of the decrease was exponential however the exponent value is small and the trend can be also represented by linear decreasing curve.
- The strain value at the crack tip of the CT specimens were observed using DIC. It was also observed that the strain at failure was also decreasing with respect to gamma irradiation.
- The values of fracture toughness in the longitudinal direction was observed to be lower than those in the transverse direction due to the crack path which is parallel to the osteons and so the resistance is lower in longitudinal CT specimen.

7.2. Future recommendations

This research may be extended in future considering the following recommendations.

- X-rays are also utilized for the sterilization of bone grafts. In similar research the effect of X-rays on hip bone may be also investigated.
- Mechanism of the effect on the decrease of mechanical properties w.r.t gamma irradiation may be investigated.

References

[1] Keaveny, T. M., Morgan, E. F., & Yeh, O. C. (2004). Bone mechanics. Standard handbook of biomedical engineering and design, 1-24.

[2] Gong, J. K., Arnold, J. S., & Cohn, S. H. (1964). Composition of trabecular and cortical bone. The Anatomical Record, 149(3), 325-331.

[3] Lowenstam, H. A., & Weiner, S. (1989). On biomineralization. Oxford University Press.

[4] Herring, G. M. (2012). The organic matrix of bone. The biochemistry and physiology of bone, 1, 127-189.

[5] Hodge, A. J., & Petruska, J. A. (1963). Recent studies with the electron microscope on ordered aggregates of the tropocollagen molecule. Aspects of protein structure, 289-300.

[6] Weiner, S., Traub, W., & Wagner, H. D. (1999). Lamellar bone: structure function relations. Journal of structural biology, 126(3), 241-255.

[7] Philip Tate. (2012). Principles of Anatomy and Physiology, 2nd Ed. Chapter 7, Anatomy of Bones and Joints. Retrieved from Mc Graw Hill online Learning center : http://highered.mheducation.com/sites/dl/free/0073378194/885148/Ch07.pdf.

[8] Martini, F. H. (2004). Fundamentals of anatomy and physiology (6th Ed.). New Jersey, USA: Prentice Hall, 182-207.

[9] Maribe, E. N. (2004). Human anatomy and physiology (6th Ed.). California, USA: Benjamin/Cummings Publishing Company Inc, 175-201.

[10] Lin, Z. X., Xu, Z. H., An, Y. H., & Li, X. (2016). In situ observation of fracture behavior of canine cortical bone under bending. Materials Science and Engineering: C, 62, 361-367.

[11] Fratzl, P., Gupta, H. S., Paschalis, E. P., & Roschger, P. (2004). Structure and mechanical quality of the collagen–mineral nano-composite in bone. Journal of materials chemistry, 14(14), 2115-2123.

[12] Bandyopadhyay-Ghosh, S. (2008). Bone as a collagen-hydroxyapatite composite and its repair. Trends Biomater Artif Organs, 22(2), 116-124.

[13] Hull, D., & Clyne, T. W. (1996). An introduction to composite materials. Cambridge university press.

[14] Cowin, S. C. (2001). Bone mechanics handbook. CRC press.

[15] Wang, X., & Puram, S. (2004). The toughness of cortical bone and its relationship with age. Annals of biomedical engineering, 32(1), 123-135.

[16] Alberts.(1994).Molecular biology of the cell. Garland Press, 3rd Ed.

[17] Rho, J. Y., Kuhn-Spearing, L., & Zioupos, P. (1998). Mechanical properties and the hierarchical structure of bone. Medical engineering & physics, 20(2), 92-102.

[18] Martin, R. B., Burr, D. B., & Sharkey, N. A. (1998). Skeletal tissue mechanics (Vol. 190). New York: Springer.

[19] Parkinson, I. H., & Fazzalari, N. L. (2013). Characterisation of trabecular bone structure. In Skeletal Aging and Osteoporosis. Berlin, Heidelberg: Springer.

[20] Currey, J. D, (2002), Bones structure and mechanics, Princeton University Press.

[21] Carola, R., Harley,J.P., Noback R.C. (1992). Human anatomy and physiology (2nd Ed.), New York, Mc Graw hill Inc.

[22] Anthony., Kolthoff. (1975). Anatomy and physiology (9th Ed). Mosby.

[23] Elaine, n., Marieb. (2000). Essentials of human anatomy and physiology (6th Ed), San Francisco, Addison welsey longmani Inc.

[24] Memmler., Lundeen, R., Barbara., Jansen ,C., Dena, L.W. (1996). The Human Body in Health and Disease (8th Ed).

[25] Pearce, J. M. S. (2009). Henry Gray's anatomy. Clinical Anatomy, 22(3), 291-295.

[26] MSU envirmental health and safety.(2013, October). Radiation safety manual . Retrievd from MSU website: www.ehs.msu.edu/radiation/programs_guidelines/radmanual/radmanual.pdf .

[27] Murray, R., & Holbert, K. E. (2014). Nuclear energy: an introduction to the concepts, systems, and applications of nuclear processes. Elsevier.

[28] Hyper Physics. Radioactivity. Retrieved from: http://hyperphysics.phy-astr.gsu.edu/hbase/Nuclear/radact.html.

[29] Mirion Technologies. Types of Ionizing Radiation . Retrieved from: https://www.mirion.com/introduction-to-radiation-safety/types-of-ionizing-radiation/.

[30] A guide to nuclear scineces. Radioactivity.Retrieved from: http://www2.lbl.gov/abc/wallchart/teachersguide/pdf/Chap03.pdf.

[31] Canadian Nuclear Safety Commission. (2012, Dec). Introduction to Radiation . Retrived from:

http://nuclearsafety.gc.ca/eng/pdfs/Reading-Room/radiation/Introduction-to-Radiation-eng.pd.

[32] IAEC. Radiation, people and environment. Retrieved from: https://www.iaea.org/sites/default/files/radiation0204.pdf.

33] Murray, R., & Holbert, K. E. (2014). Nuclear energy: an introduction to the concepts, systems, and applications of nuclear processes. Elsevier.

[34] Molins, R. A. (2001). Food irradiation: principles and applications. John Wiley & Sons.

[35] Nguyen, H., Morgan, D. A., & Forwood, M. R. (2007). Sterilization of allograft bone: effects of gamma irradiation on allograft biology and biomechanics. Cell and tissue banking, 8(2), 93-105.

[36] Kennedy, J. F., Phillips, G. O., & Williams, P. A. (2005). Sterilisation of tissues using ionizing radiations. CRC Press.

[37] Barth, H. D., Zimmermann, E. A., Schaible, E., Tang, S. Y., Alliston, T., & Ritchie, R. O. (2011). Characterization of the effects of x-ray irradiation on the hierarchical structure and mechanical properties of human cortical bone. Biomaterials, 32(34), 8892-8904.

[38] Barth, H. D., Launey, M. E., MacDowell, A. A., Ager, J. W., & Ritchie, R. O. (2010). On the effect of X-ray irradiation on the deformation and fracture behavior of human cortical bone. Bone, 46(6), 1475-1485.

[39] Russell, N. A., Pelletier, M. H., Bruce, W. J., & Walsh, W. R. (2012). The effect of gamma irradiation on the anisotropy of bovine cortical bone. Medical engineering & physics, 34(8), 1117-1122.

[40] Gehron, R. P. (1989). The biochemistry of bone. Endocrinology and metabolism clinics of North America, 18(4), 858-902.

[41] Burton, B., Gaspar, A., Josey, D., Tupy, J., Grynpas, M. D., & Willett, T. L. (2014). Bone embrittlement and collagen modifications due to high-dose gamma-irradiation sterilization. Bone, 61, 71-81.

[42] Singhal, A., Deymier-Black, A. C., Almer, J. D., & Dunand, D. C. (2011). Effect of high-energy X-ray doses on bone elastic properties and residual strains. Journal of the mechanical behavior of biomedical materials, 4(8), 1774-1786.

[43] Gibbons, M. J., Butler, D. L., Grood, E. S., Bylski-Austrow, D. I., Levy, M. S., & Noyes, F. R. (1991). Effects of gamma irradiation on the initial mechanical and material

properties of goat bone-patellar tendon-bone allografts. Journal of Orthopaedic Research, 9(2), 209-218.

[44] Tüfekci, K., Kayacan, R., & Kurbanoğlu, C. (2014). Effects of gamma radiation sterilization and strain rate on compressive behavior of equine cortical bone. Journal of the mechanical behavior of biomedical materials, 34, 231-242.

[45] Balsly, C. R., Cotter, A. T., Williams, L. A., Gaskins, B. D., Moore, M. A., & Wolfinbarger Jr, L. (2008). Effect of low dose and moderate dose gamma irradiation on the mechanical properties of bone and soft tissue allografts. Cell and tissue banking, 9(4), 289-298.

[46] Akkus, O., & Rimnac, C. M. (2001). Fracture resistance of gamma radiation sterilized cortical bone allografts. Journal of Orthopaedic Research, 19(5), 927-934.

[47] Vastel, L., Meunier, A., Siney, H., Sedel, L., & Courpied, J. P. (2004). Effect of different sterilization processing methods on the mechanical properties of human cancellous bone allografts. Biomaterials, 25(11), 2105-2110.

[48] Dux, S. J., Ramsey, D., Chu, E. H., Rimnac, C. M., & Hernandez, C. J. (2010). Alterations in damage processes in dense cancellous bone following gamma-radiation sterilization. Journal of biomechanics, 43(8), 1509-1513.

[49] Salehpour, A., Butler, D. L., Proch, F. S., Schwartz, H. E., Feder, S. M., Doxey, C. M., & Ratcliffe, A. (1995). Dose-dependent response of gamma irradiation on mechanical properties and related biochemical composition of goat bone-patellar tendon-bone allografts. Journal of orthopaedic research, 13(6), 898-906.

[50] Anderson, M. J., Keyak, J. H., & Skinner, H. B. (1992). Compressive mechanical properties of human cancellous bone after gamma irradiation. J Bone Joint Surg Am, 74(5), 747-752.

[51] Fideler, B. M., Vangsness JR, C. T., Lu, B., Orlando, C., & Moore, T. (1995). Gamma irradiation: effects on biomechanical properties of human bone-patellar tendon-bone allografts. The American Journal of Sports Medicine, 23(5), 643-646.

[52] Currey, J. D., Foreman, J., Laketić, I., Mitchell, J., Pegg, D. E., & Reilly, G. C. (1997). Effects of ionizing radiation on the mechanical properties of human bone. Journal of orthopaedic research, 15(1), 111-117.

[53] Astm, E. (1991). 399-90:" Standard test method for plane-strain fracture toughness of metallic materials. Annual book of ASTM standards, 3(01), 506-536.

[54] Pan, B., Qian, K., Xie, H., & Asundi, A. (2009). Two-dimensional digital image correlation for in-plane displacement and strain measurement: a review. Measurement science and technology, 20(6), 1-17.

[55] Zhang, D., & Arola, D. D. (2004). Applications of digital image correlation to biological tissues. Journal of Biomedical Optics, 9(4), 691-699.

[56] Norman, T. L., Vashishth, D., & Burr, D. B. (1995). Fracture toughness of human bone under tension. Journal of biomechanics, 28(3), 309-320.

[57] Standard, A. S. T. M. (1995). Standard test method for tensile properties of polymer matrix composite materials. ASTM D3039/D 3039M.

[58] Hamer, A. J., Strachan, J. R., Black, M. M., Ibbotson, C. J., Stockley, I., & Elson, R. A. (1996). Biomechanical properties of cortical allograft bone using a new method of bone strength measurement. Bone & Joint Journal, 78(3), 363-368.

[59] Hernigou, P., Gras, G., Marinello, G., & Dormont, D. (2000). Inactivation of HIV by application of heat and radiation: implication in bone banking with irradiated allograft bone. Acta orthopaedica Scandinavica, 71(5), 508-512.

[60] Loty, B., Courpied, J. P., Tomeno, B., Postel, M., Forest, M., & Abelanet, R. (1990). Bone allografts sterilised by irradiation. International orthopaedics, 14(3), 237-242.